

‘Maximum information’ crystal calorimetry for e^+e^- colliders



HKUST JOCKEY CLUB
INSTITUTE FOR ADVANCED STUDY

IAS PROGRAM

Online Program

High Energy Physics

January 14-21, 2021

20/01/21

W.Chung¹, S.Eno², Y.Lai²,

M.Lucchini¹, C.Tully¹

¹Princeton University

²University of Maryland

‘Maximum information’ crystal calorimetry for e^+e^- colliders



Excellent energy resolution to photons and neutral hadrons
($\sim 3\%/\sqrt{E}$ and $\sim 30\%/\sqrt{E}$ respectively)

Separate readout of scintillation and Cherenkov light
(for integration with a dual-readout hadron calorimeter)

Longitudinal and transverse segmentation
(to provide more handles for particle flow algorithms)

Precise time tagging for both MIPs and EM showers
(time resolution better than 30 ps)

Overview of the talk

- Some **examples to exploit a $3\%/\sqrt{E}$ energy resolution for photons**
(π^0 clustering, jet reconstruction, Brem recovery)
- **Optimization of a hybrid segmented calorimeter concept** achieving the highest resolution for both photons [$\sim 3\%/\sqrt{E}$] and neutral hadrons [$< 30\%/\sqrt{E}$]
- **Potential for particle identification**

More details about this talk in:
<https://doi.org/10.1088/1748-0221/15/11/P11005>



PUBLISHED BY IOP PUBLISHING FOR SISSA MEDIALAB

RECEIVED: August 4, 2020

REVISED: September 11, 2020

ACCEPTED: September 15, 2020

PUBLISHED: November 2, 2020

New perspectives on segmented crystal calorimeters for future colliders

M.T. Lucchini,^{a,1} W. Chung,^a S.C. Eno,^b Y. Lai,^b L. Lucchini,^c M. Nguyen^a and C.G. Tully^a

^aPrinceton University,
Princeton, New Jersey, U.S.A.

^bUniversity of Maryland,
College Park, Maryland, U.S.A.

^cFondazione Bruno Kessler,
Trento, Italy

E-mail: marco.lucchini@cern.ch

ABSTRACT: Crystal calorimeters have a long history of pushing the frontier on high-resolution electromagnetic (EM) calorimetry for photons and electrons. We explore in this paper major innovations in collider detector performance that can be achieved with crystal calorimetry when longitudinal segmentation and dual-readout capabilities are combined with a new high EM resolution approach to Particle Flow in multi-jet events, such as $e^+e^- \rightarrow HZ$ events in all-hadronic final-states at Higgs factories. We demonstrate a new technique for pre-processing π^0 momenta through combinatoric di-photon pairing in advance of applying jet algorithms. This procedure significantly reduces π^0 photon splitting across jets in multi-jet events. The correct photon-to-jet assignment efficiency improves by a factor of about 3 when the EM resolution is improved from 15 to $3\%/\sqrt{E}$. In addition, the technique of bremsstrahlung photon recovery significantly improves electron momentum measurements. A high EM resolution calorimeter increases the Z boson recoil mass resolution in Higgsstrahlung events for decays into electron pairs to 80% of that for muon pairs. We present the design and optimization of a highly segmented crystal detector concept that achieves the required energy resolution of $3\%/\sqrt{E}$, and a time resolution better than 30 ps providing exceptional particle identification capabilities. We demonstrate that, contrary to previous detector designs that suffered from large neutral hadron resolution degradation from one interaction length of crystals in front of a sampling hadron calorimeter, the implementation of dual-readout on crystals permits to achieve a resolution better than $30\%/\sqrt{E} \oplus 2\%$ for neutral hadrons. Our studies find that the integration of crystal calorimetry into future Higgs factory collider detectors can open new perspectives by yielding the highest level of combined EM and neutral hadron resolution in the PFA paradigm.

Final States of e^+e^- Higgs Physics @~246 GeV

- SM Higgs

- **0 jets: 3%:** $Z \rightarrow ll, \nu\nu$ (30%); $H \rightarrow 0 \text{ jets}$ (~10%, $\tau\tau, \mu\mu, \gamma\gamma, \gamma Z/WW/ZZ \rightarrow \text{leptonic}$)

- **2 jets: 32%**

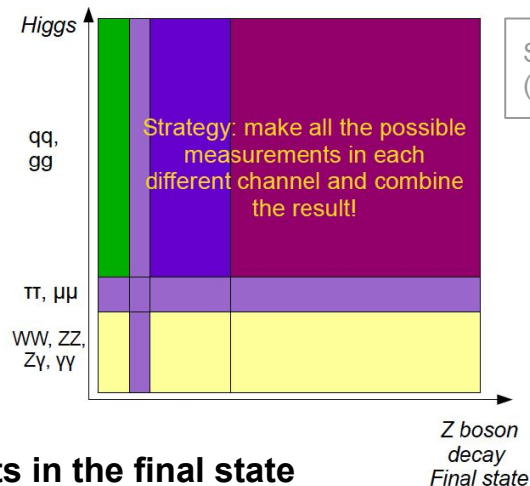
- $Z \rightarrow qq, H \rightarrow 0 \text{ jets}$. $70\% \cdot 10\% = 7\%$
 - $Z \rightarrow ll, \nu\nu; H \rightarrow 2 \text{ jets}$. $30\% \cdot 70\% = 21\%$
 - $Z \rightarrow ll, \nu\nu; H \rightarrow WW/ZZ \rightarrow \text{semi-leptonic}$. 3.6%

- **4 jets: 55%**

- $Z \rightarrow qq, H \rightarrow 2 \text{ jets}$. $70\% \cdot 70\% = 49\%$
 - $Z \rightarrow ll, \nu\nu; H \rightarrow WW/ZZ \rightarrow 4 \text{ jets}$. $30\% \cdot 15\% = 4.5\%$

- **6 jets: 11%**

- $Z \rightarrow qq, H \rightarrow WW/ZZ \rightarrow 4 \text{ jets}$. $70\% \cdot 15\% = 11\%$



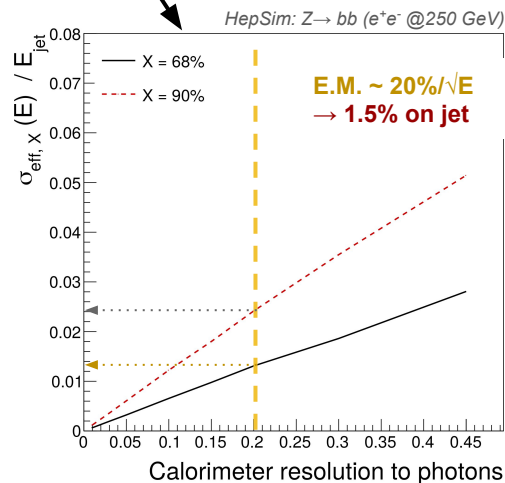
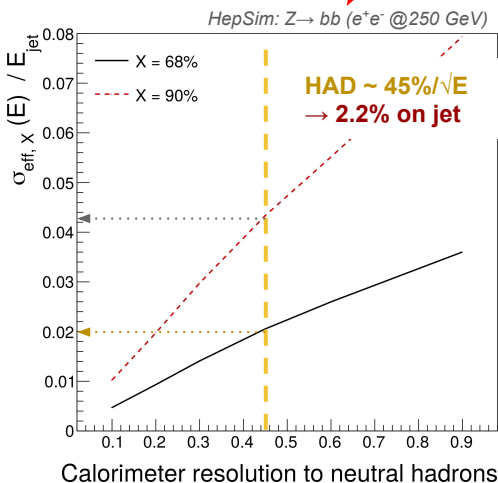
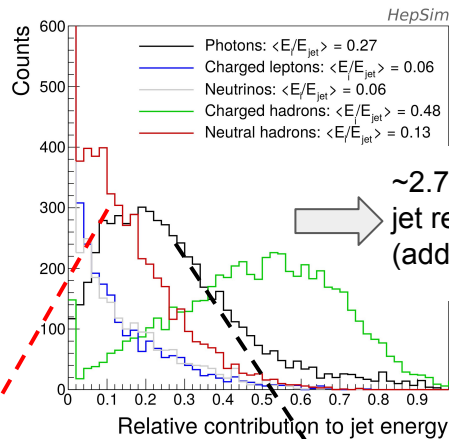
- **97% of the SM Higgsstrahlung signal has jets in the final state**

- **1/3** has only 2 jets
 - **2/3** need color-single identification (grouping the hadronic final state particles into color-singlets)

Jet resolution is a key benchmark for e^+e^- detectors performance

Traditional impact of calorimeters on jet resolution

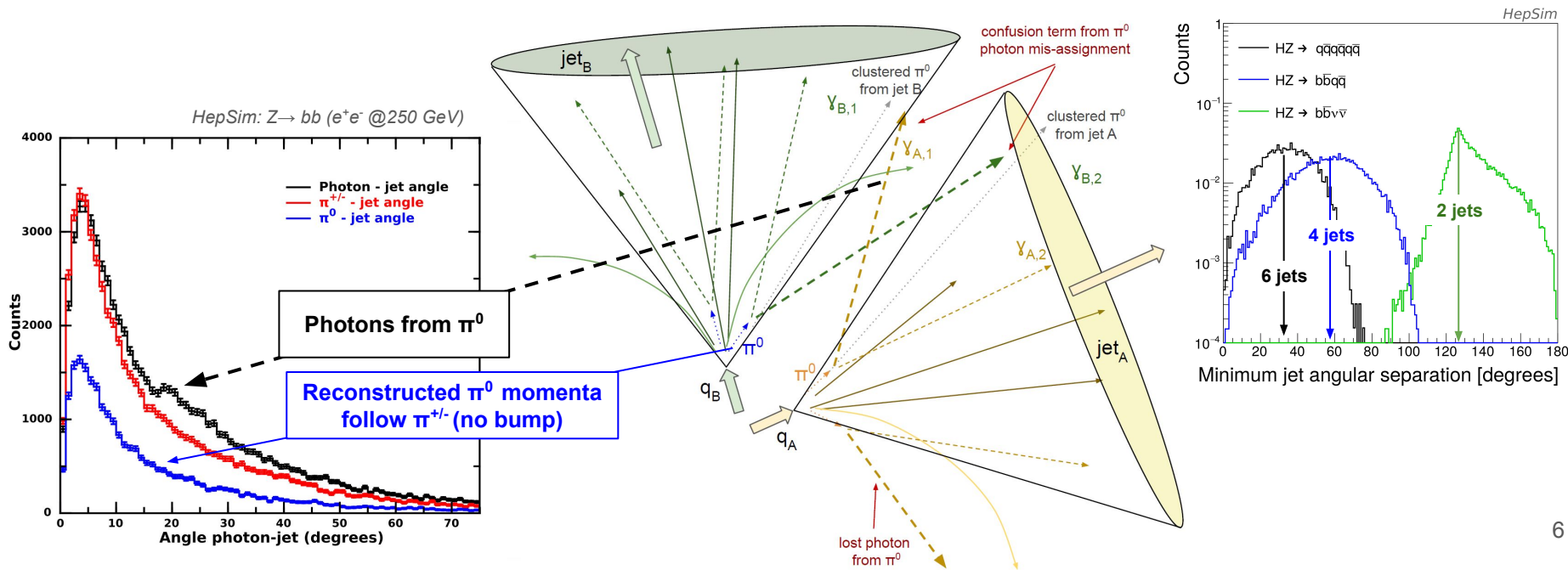
- Baseline jet performance depends on particle composition and the relevant sub-detector resolutions
- Calorimeter resolution on neutral particles required to achieve target jet resolution of $\sim 3\%$
 - **Photons**
better than $20\%/\sqrt{E}$
 - **Neutral hadrons**
(mostly $K^{0,L}$ of $\langle E \rangle \sim 5$ GeV) better than $45\%/\sqrt{E}$



But the role of calorimeters in jet reconstruction spans beyond the direct impact on energy resolution...

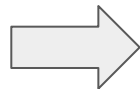
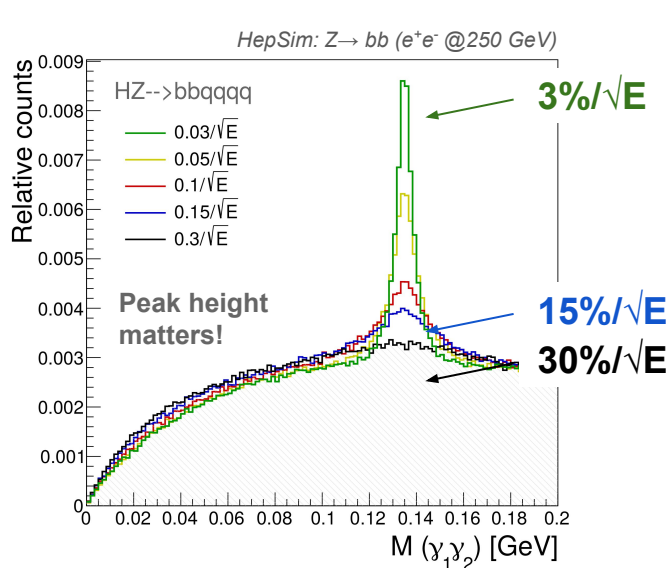
High photon resolution potential for PFA

- Many photons from π^0 decay are emitted at a $\sim 20\text{-}35^\circ$ angle wrt to the jet momentum and can get scrambled across neighboring jets
- Effect particularly pronounced in 4 and 6 jets topologies

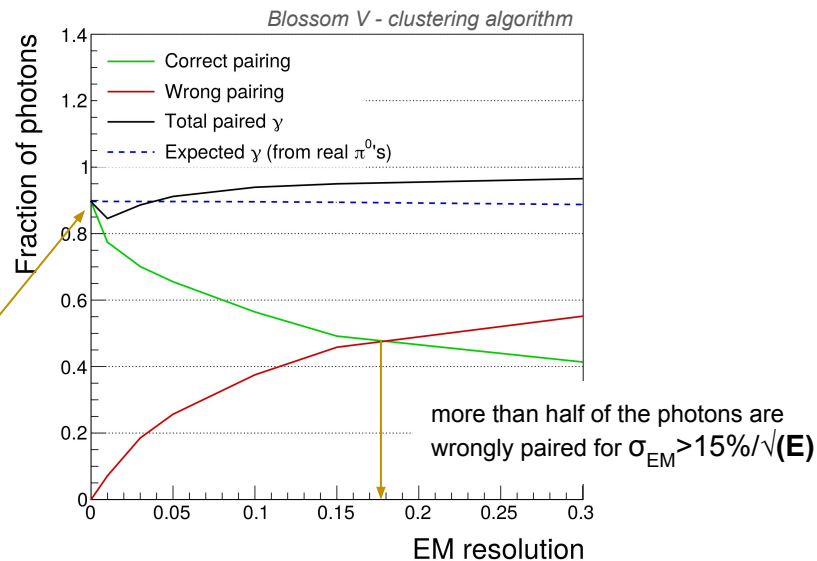


A graph-based algorithm for π^0 clustering

- A high EM resolution enables efficient clustering of photons from π^0 's
 - Large fraction of π^0 photons correctly clustered with good σ_{EM}
 - **~90% for ~3%/√(E)** vs **50% for ~30%/√(E)**
 - Large fraction of “fake π^0 ’s” reconstructed with poor σ_{EM}
 - **~50% for ~30%/√(E)** vs **10% with ~3%/√(E)**

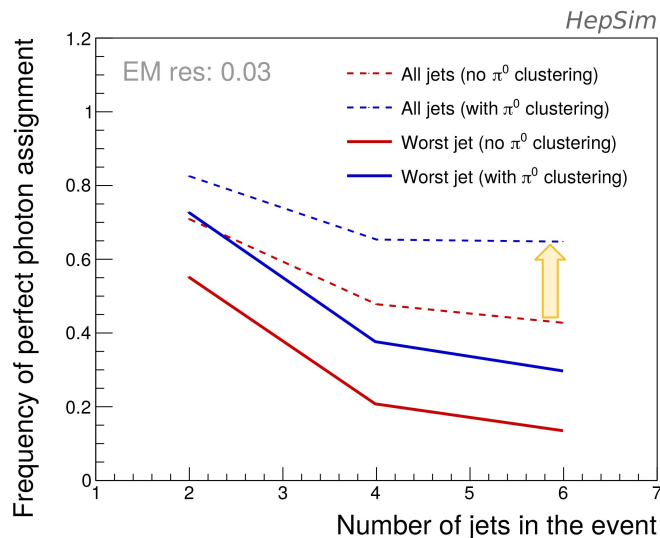
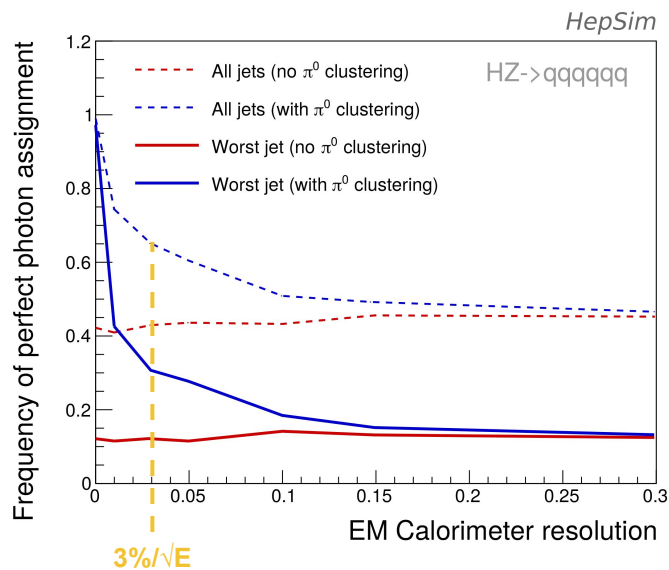


perfect clustering
for perfect energy
measurement



Improvements in photon-to-jet correct assignment

- **High e.m. resolution enables** photons clustering into π^0 's by reducing their angular spread with respect to the corresponding jet momentum
- **Improvements in the fraction of photons correctly clustered to a jet** sizable only for e.m. resolutions of $\sim 3\%/\sqrt{(E)}$

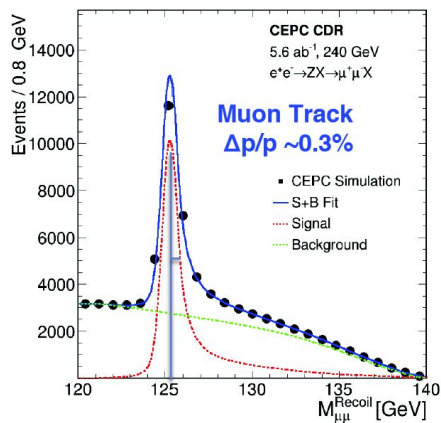


Recovery of Bremsstrahlung photons

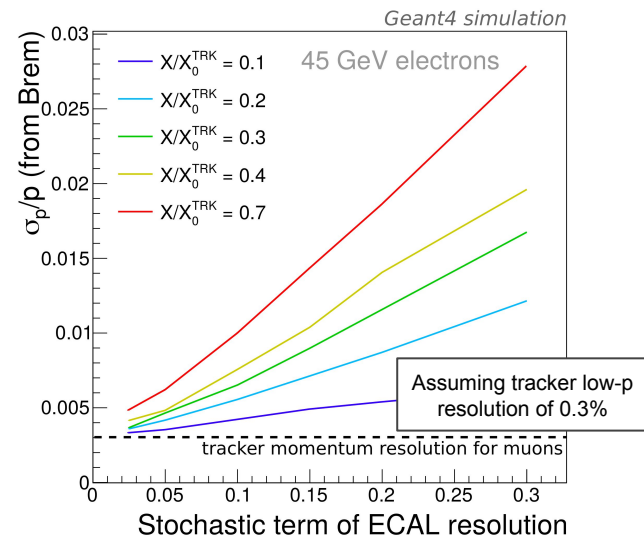
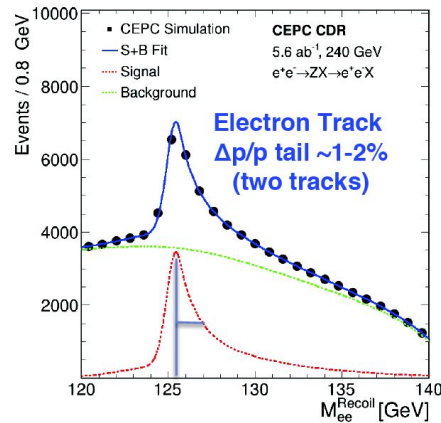
- Reconstruction of the Higgs boson mass and width from the recoil mass of the Z boson is a key tool at e^+e^- colliders
- Potential to **improve the resolution of the recoil mass signal from $Z \rightarrow ee$ decays** to about 80% of that from $Z \rightarrow \mu\mu$ decays [with Brem photon recovery at EM resolution of $3\%/\sqrt{E}$]

Example from [CEPC CDR](#)

► $Z \rightarrow \mu^+\mu^-$ Recoil



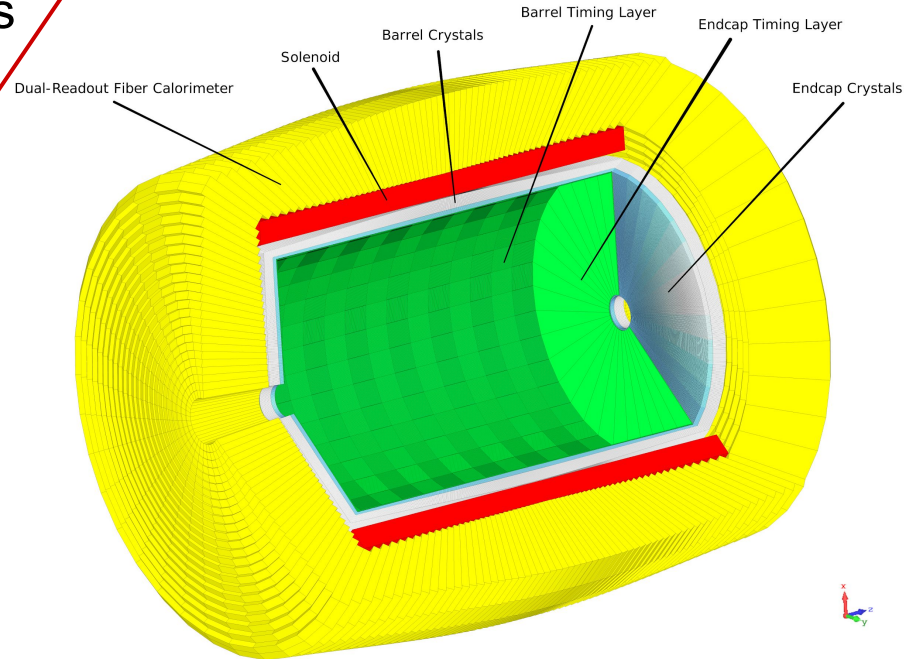
► $Z \rightarrow e^+e^-$ Recoil



~80% of resolution recovery
with $3\%/\sqrt{E}$

The combination of a **segmented crystal high precision EM calorimeter (SCEPCal)** with a **dual-readout hadron calorimeter** would be *IDEAL* to take up the challenge of precision physics at future e^+e^- colliders

- Design optimization of a segmented crystal ECAL
- Effective integration with a dual-readout HCAL
- Global cost-performance optimization



Layout overview

- **Transverse and longitudinal segmentations** optimized for particle identification and particle flow algorithms
- Exploiting **SiPM readout** for contained cost and power budget

- **Timing layers** • $\sigma_t \sim 20 \text{ ps}$

- LYSO:Ce crystals ($\sim 1X_0$)
- $3 \times 3 \times 60 \text{ mm}^3$ active cell
- $3 \times 3 \text{ mm}^2$ SiPMs (15-20 μm)

- **ECAL layers** • $\sigma_E^{\text{EM}}/E \sim 3\%/\sqrt{E}$

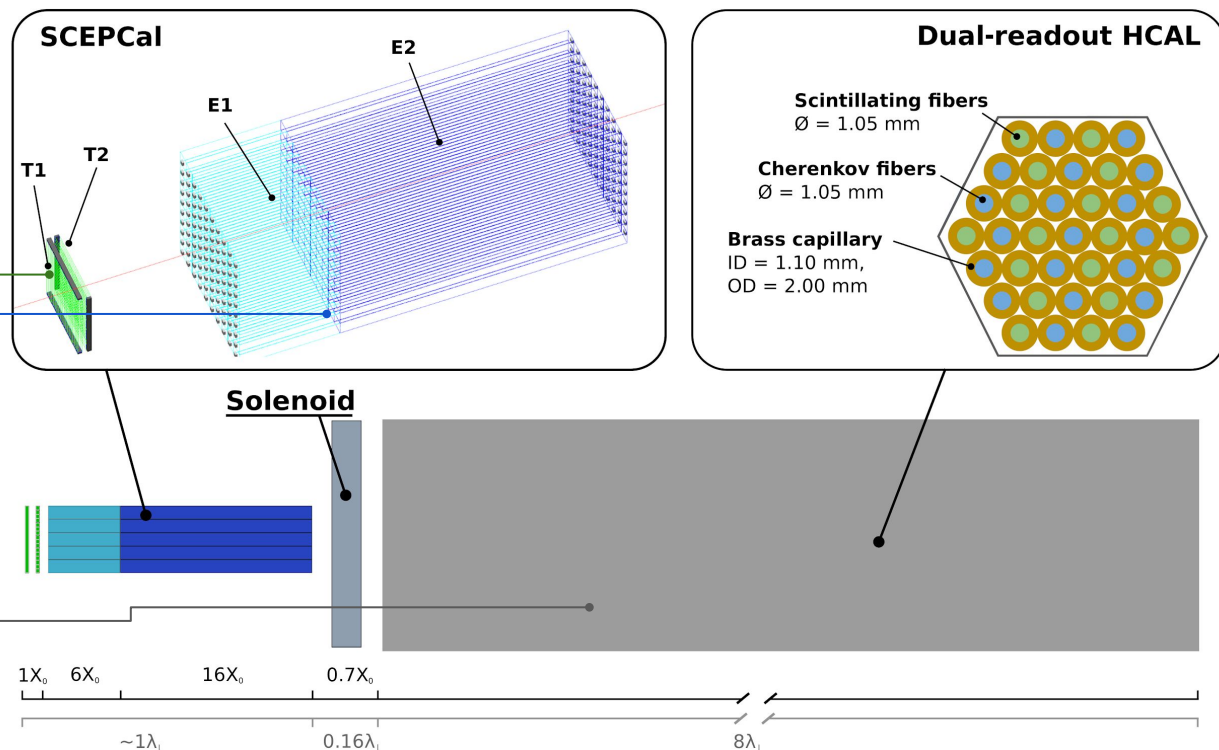
- PWO crystals
- **Front segment** ($\sim 6X_0$)
- **Rear segment** ($\sim 16X_0$)
- $10 \times 10 \times 200 \text{ mm}^3$ crystal
- $5 \times 5 \text{ mm}^2$ SiPMs (10-15 μm)

- **Ultra-thin IDEA solenoid**

- $\sim 0.7X_0$

- **HCAL layer** • $\sigma_E^{\text{HAD}}/E \sim 27\%/\sqrt{E}$

- Scintillating and quartz fibers inserted in brass capillaries (similar to prototypes in A.Karadzhinova-Ferrer [slides](#))



Some crystal options

- **PWO**: the most compact, the fastest
- BGO/BSO: parameters tunable by adjusting the Si-fraction
- Csl: the less compact, the slowest, the brightest

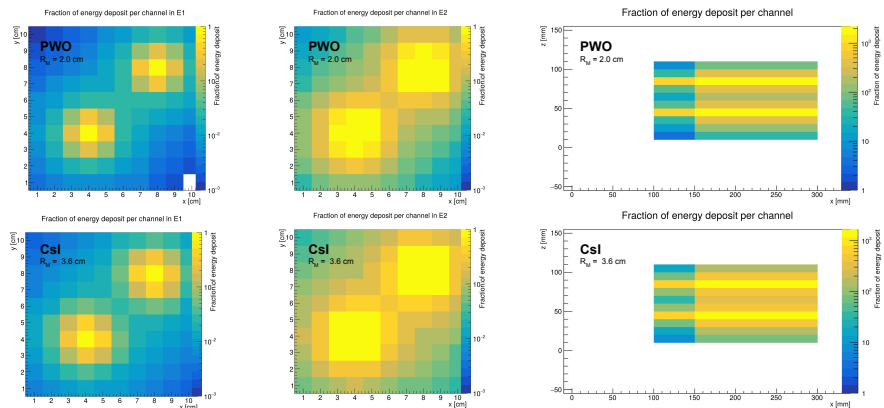
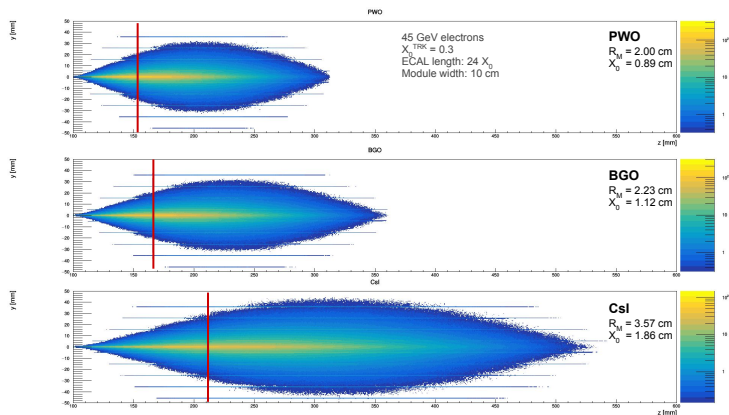
better for PFA



better stochastic term

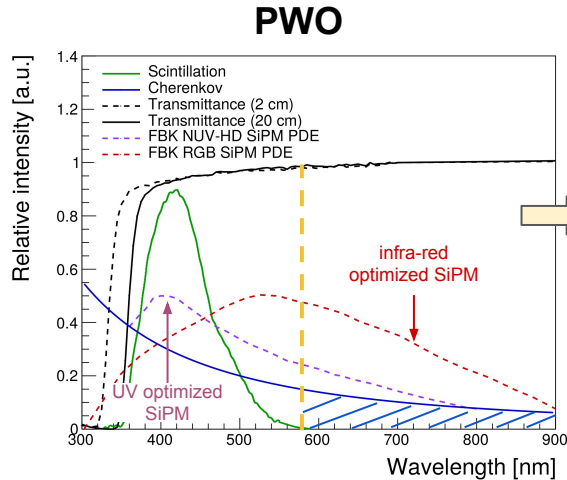
Crystal	Density g/cm ³	λ_1 cm	X_0 cm	R_M cm	Relative LY @ RT	Decay time ns	Photon density (LY / τ_D) ph/ns	dLY/dT (% / °C)	Cost (10 m ³) Est. \$/cm ²	Cost* X_0 Est. \$/cm ²
PWO	8.3	20.9	0.89	2.00	1	10	0.10	-2.5	8	7.1
BGO	7.1	22.7	1.12	2.23	70	300	0.23	-0.9	7	7.8
BSO	6.8	23.4	1.15	2.33	14	100	0.14	--	6.8	7.8
Csl	4.5	39.3	1.86	3.57	550	1220	0.45	+0.4	4.3	8.0

Working with the **Crystal Clear Collaboration** at CERN to evaluate crystal candidates for DRO

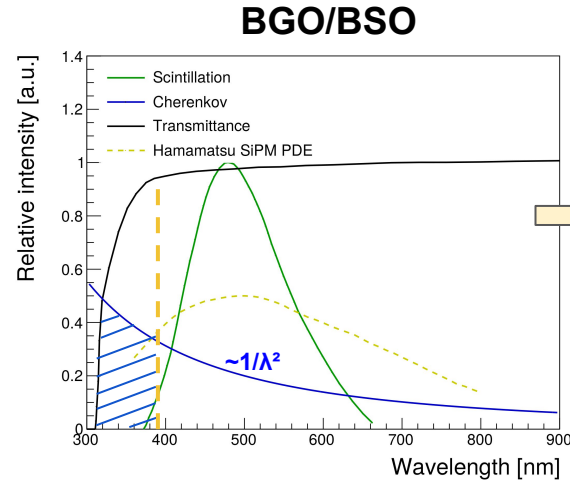


Cherenkov detection in PWO and BGO

- Sensitivity in both the UV and infrared region with Silicon Photomultipliers
- Different approaches being explored for a cost-contained ECAL with DRO capabilities:
 - Detect Cherenkov photons in either the UV (BGO) or infrared region (PWO)
 - Ongoing laboratory measurement at CERN Lab27 to validate simulation (Crystal Clear RD18)



Cherenkov photons
above scintillation peak
are much less affected
by self-absorption



BGO/BSO have larger
stokes shift, i.e. a wider
range of transparency
for 'UV Cherenkov'

Energy resolution for **EM** particles

- Contributions to energy resolution:

- Shower fluctuations

- Longitudinal leakage
- Tracker material budget
- Services for front layers readout

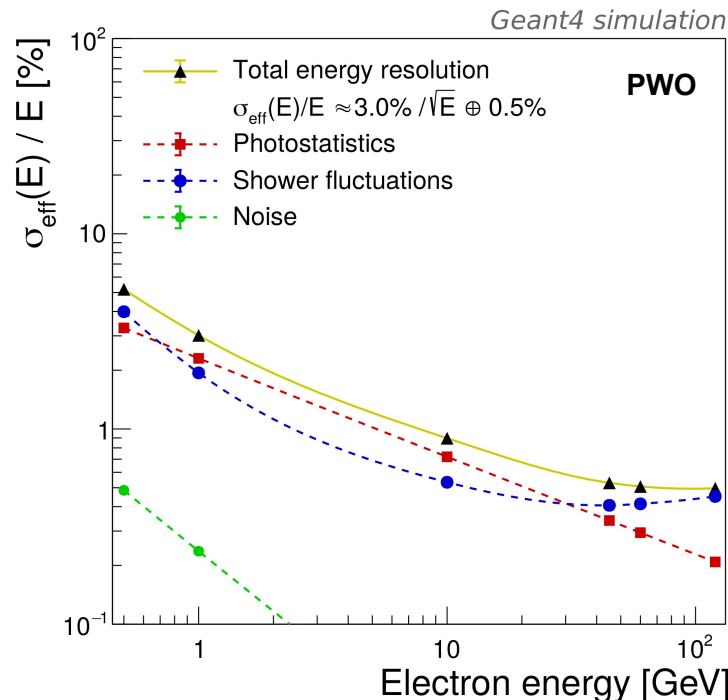
- Photostatistics

- Tunable parameter depending on:
 - SiPM choice
 - Crystal choice

- Noise

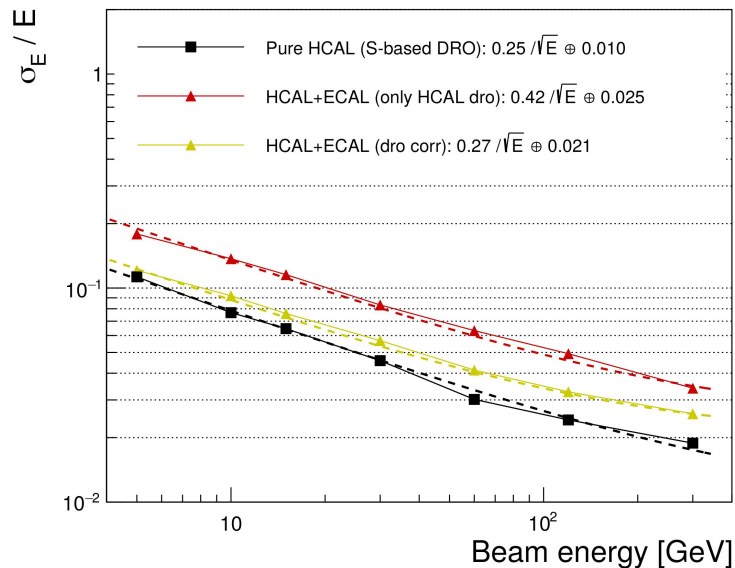
- Negligible with SiPMs
 - High gain devices ($\sim 10^5$)
 - Small dark count rate within signal integration time window

$$\sigma_E/E \sim 3\%/\sqrt{E} \oplus 0.5\%$$



Energy resolution for neutral hadrons

1. Correct the energy deposit in the HCAL with DRO
2. Correct the energy deposit in the SCEPCal with DRO
3. Calibrated sum of SCEPCal+HCAL

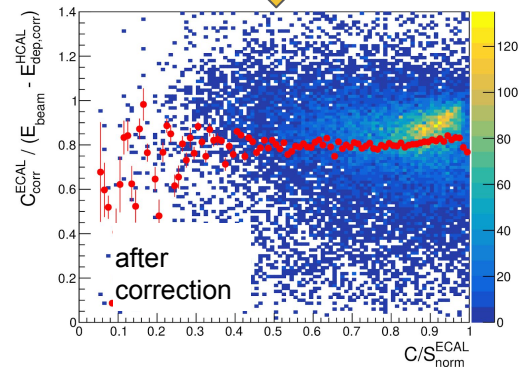
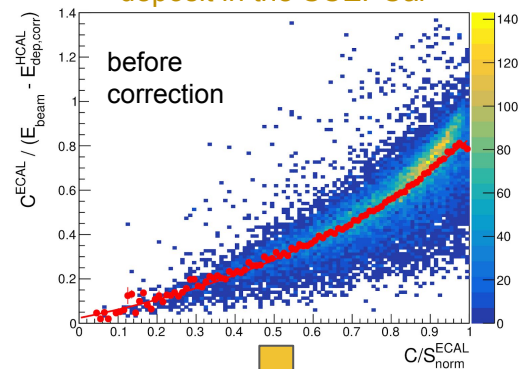


$\sim 27\%/\sqrt{E} \oplus 2\%$

Good stochastic term recovered with crystal dual readout!

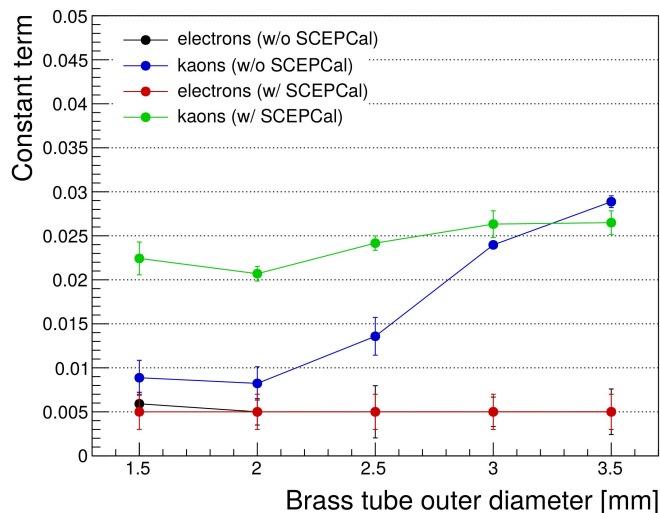
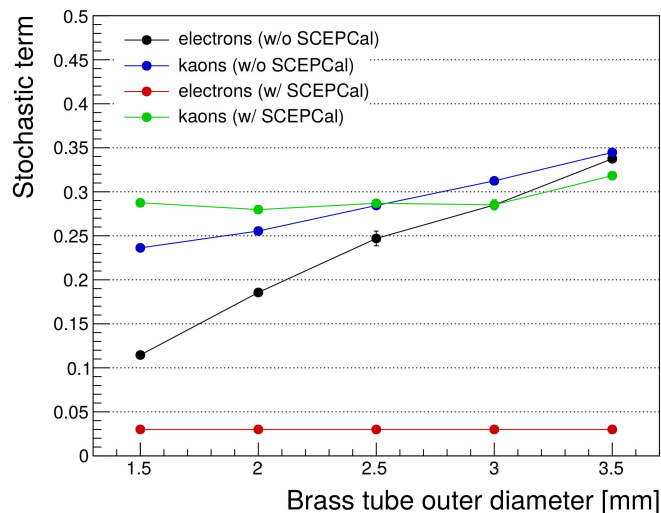
- ← adding raw SCEPCal energy
- ← adding DRO corr SCEPCal
- ← pure HCAL

DRO correction for the energy deposit in the SCEPCal

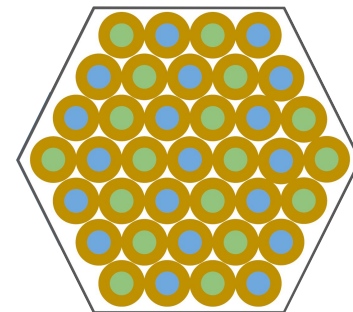


Calorimeter cost/performance optimization

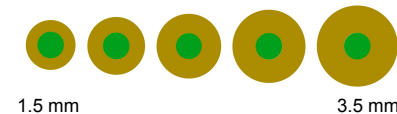
- Brass tube outer diameter (OD) can be increased to 3/3.5 mm with marginal impact on the hadron resolution
- Relative channel reduction and cost decrease approximately with $\sim 1/OD^2$



Brass capillaries
“Nominal” dimension
OD=2 mm, ID=1.1 mm

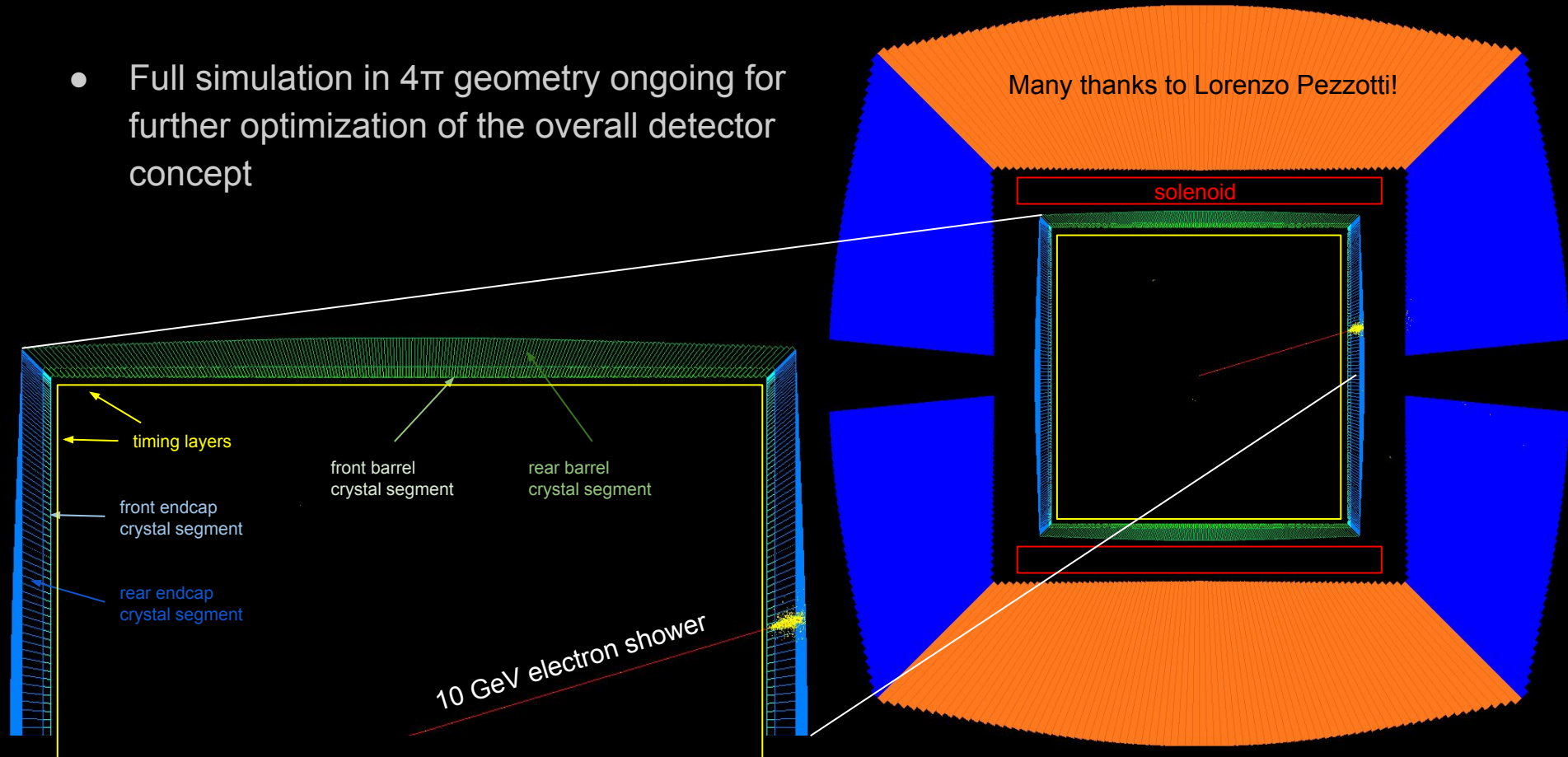


Active fiber diameter unchanged
Brass tube outer diameter varied



Ongoing integration in 4 π Geant4 IDEA simulation

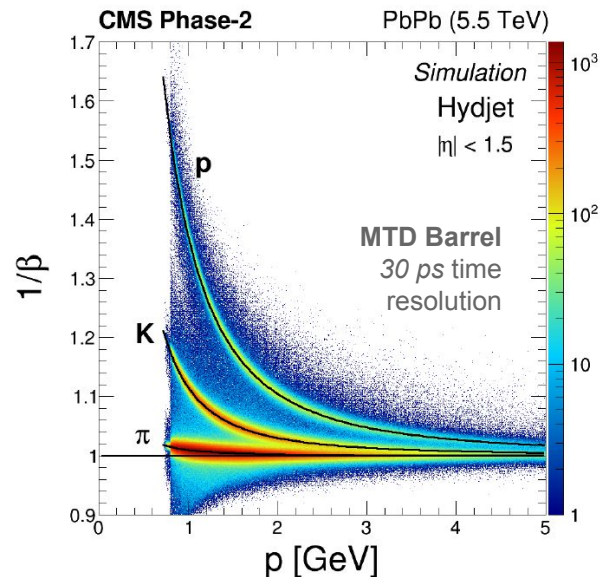
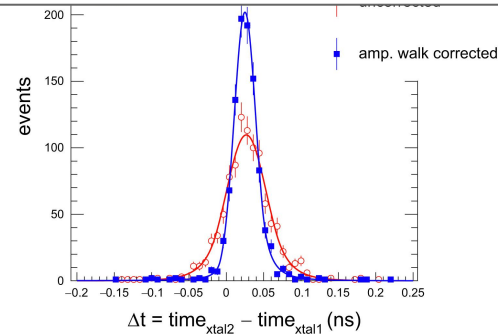
- Full simulation in 4 π geometry ongoing for further optimization of the overall detector concept



Particle ID with time-of-flight

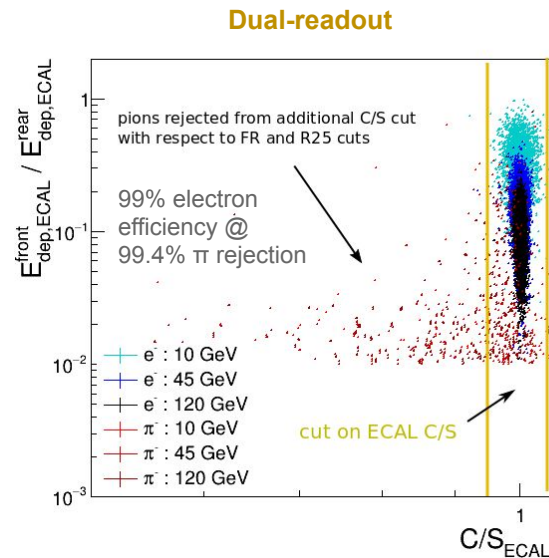
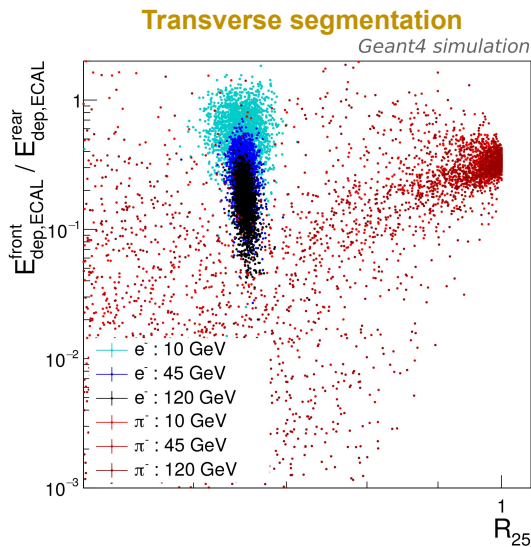
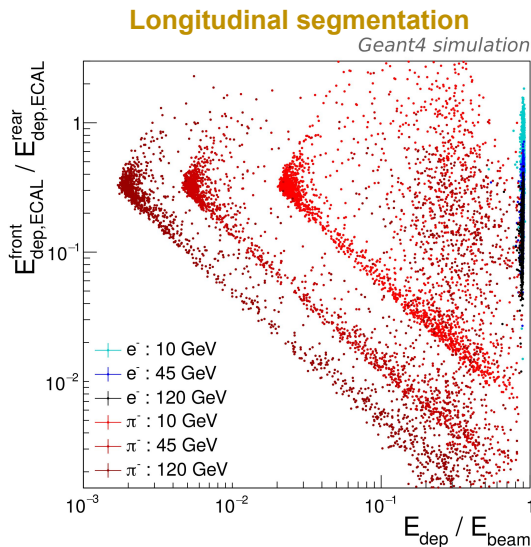
- Crystals can provide excellent timing capabilities for particle identification:
 - Time tagging of **MIPs with ~30 ps** time resolution with single layer
 - See [MTD in CMS Phase 2 upgrade](#)
 - Time resolution of **~30 ps to e.m. showers** with $E > 20$ GeV with the ECAL (rear) segment(s)
 - See [Phase 2 CMS ECAL Upgrade](#)

Time resolution to single muons with
LYSO crystals: $\sigma_t \sim 10$ ps
<https://doi.org/10.1016/j.nima.2016.05.030>



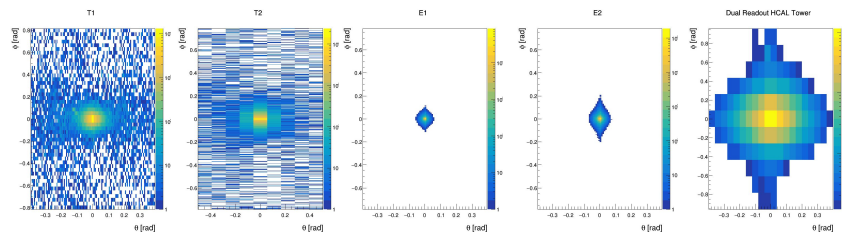
Particle ID with crystal segmentation

- Topology of longitudinal/transverse energy deposits in crystals provides a **clear $e^{+/-}/\pi^{+/-}$ discrimination** → better than 99% electron efficiency at 99% pion rejection (with simple cuts)
- **Large potential for improvement with the addition of dual-readout information** and use of more sophisticated pattern recognition algorithm

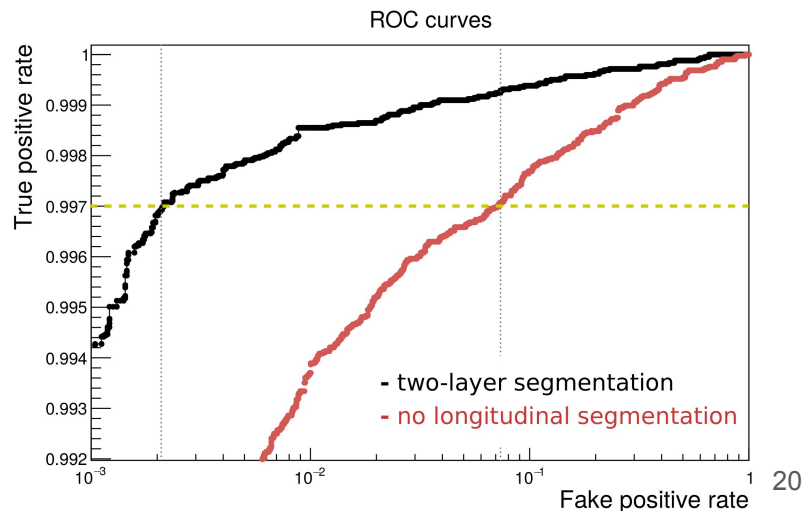


Exploiting segmentation for PID using CNNs

- Exploit the 5 calorimeter longitudinal layers:
 - For each layer the transverse segmentation combined with the additional information (e.g. dual readout and timing) can be treated as a colored image
 - Extract features from each image with convolutional filters
 - Combine features to identify particle patterns to achieve particle discrimination
- Preliminary results: **longitudinal segmentation in the crystal EM section substantially reduces pion mis-identification rate**



e^-/π^- discrimination with ECAL only



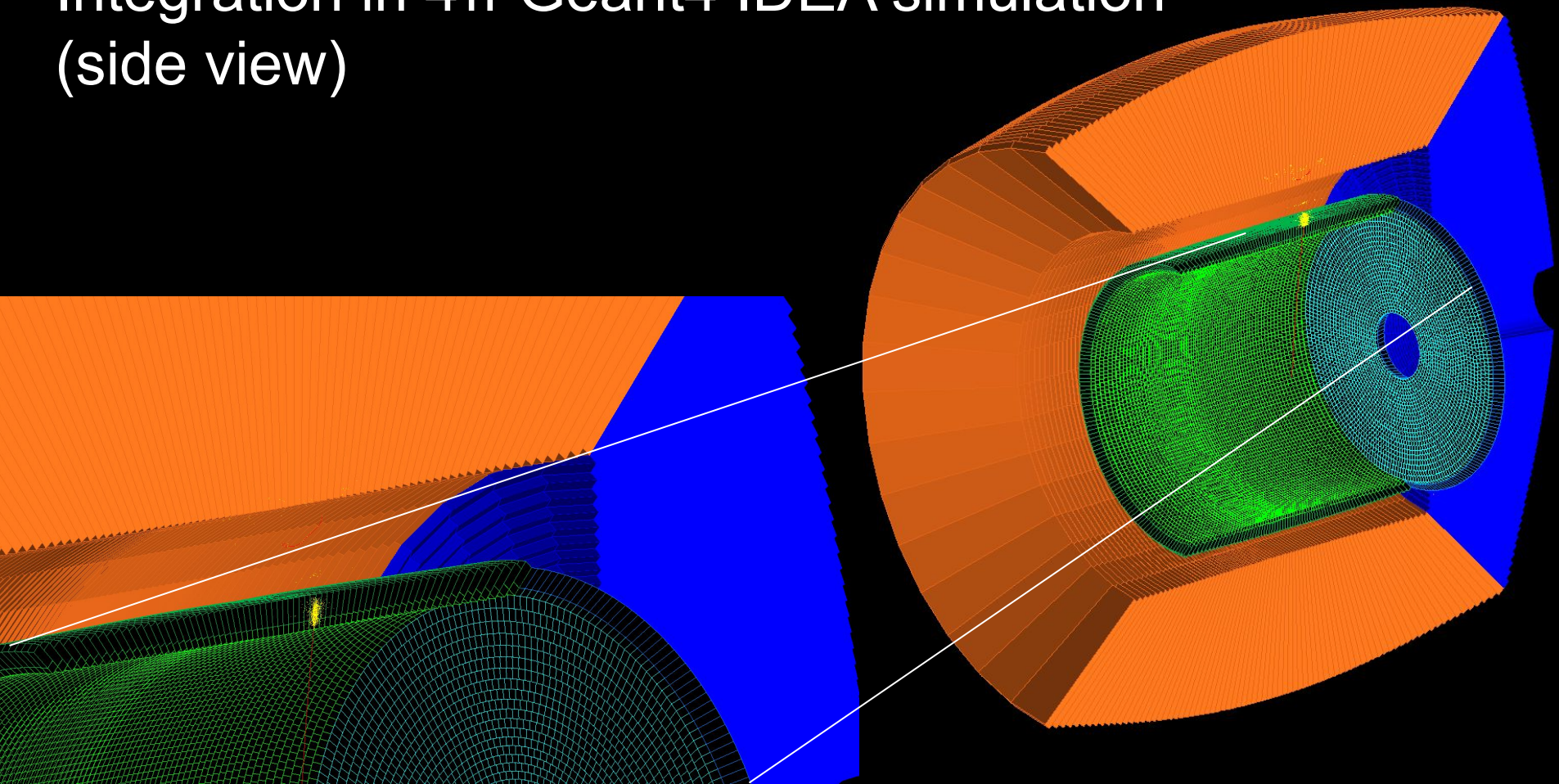
Summary

- **Highlights of a segmented crystal calorimeter with dual readout**
 - **Excellent DRO hadron calorimetry** better than $\sim 30\%/\sqrt{E}$ is maintained with a segmented crystal EM calorimeter in front of the thin solenoid in the IDEA detector
 - **Addition of $\sim 3\%/\sqrt{E}$ EM resolution** for photons and brem recovery for electrons
 - **Efficient pre-clustering of pizero photons**, improves the correct photon-to-jet assignment especially in 4 and 6 jets event topologies
- Combination of a DRO ECAL with a DRO HCAL allows for a **global optimization of** each calorimeter compartment in terms of **channel count, readout and cost**
- Exploit timing capabilities, segmentation and dual readout to **maximize the information extracted from the segmented crystals as a linchpin** to provide stronger criteria in matching to the tracking and hadron calorimeter measurements

Additional slides

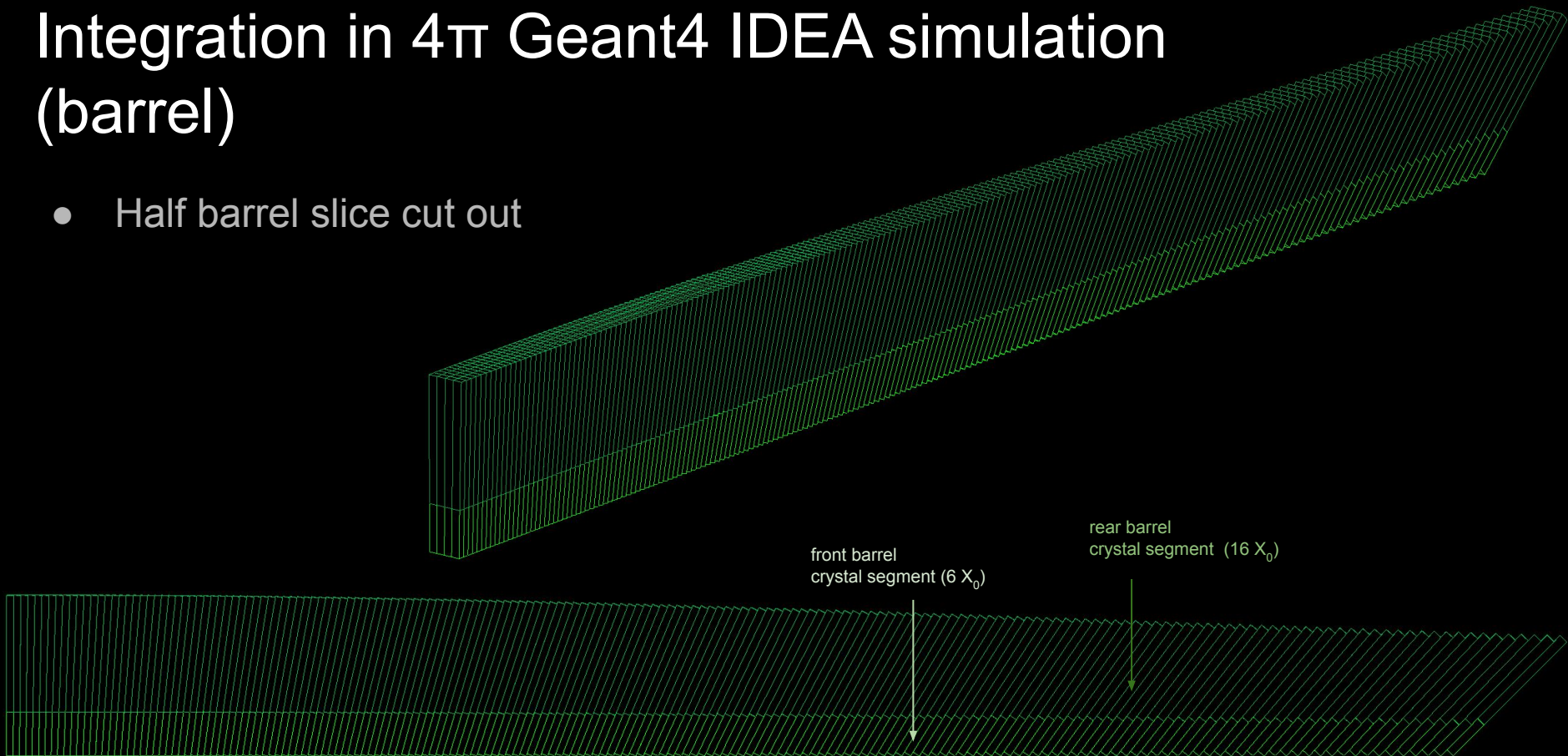
More on 4π geometry integration

Integration in 4π Geant4 IDEA simulation (side view)



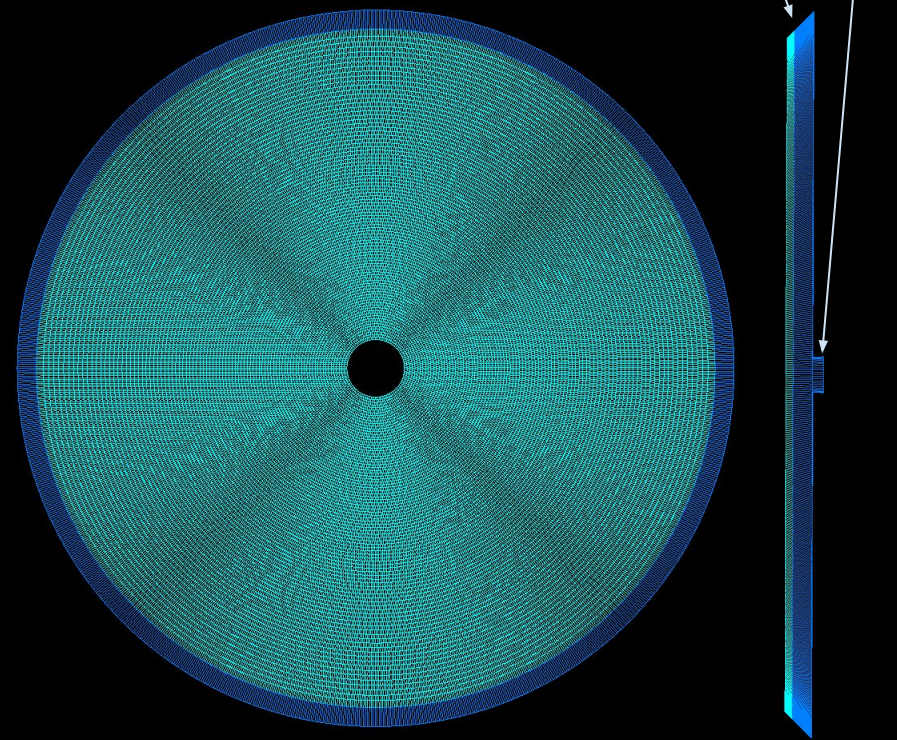
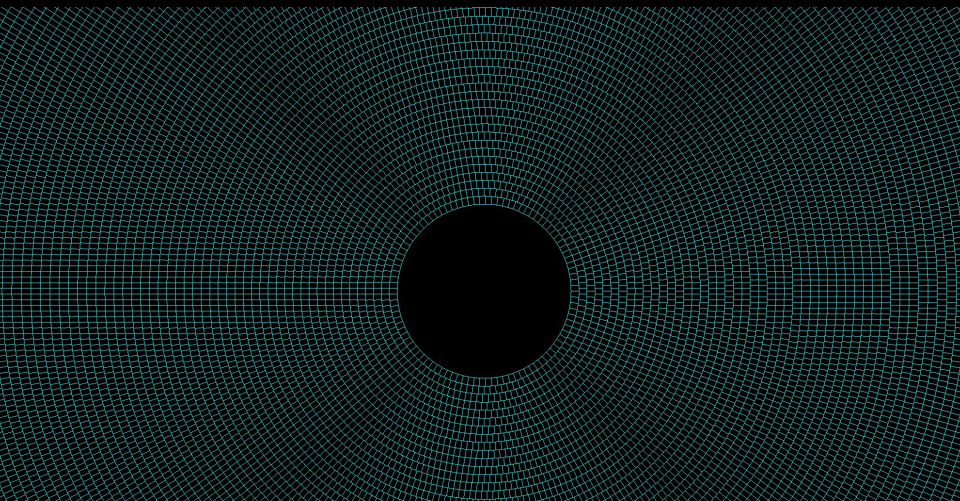
Integration in 4π Geant4 IDEA simulation (barrel)

- Half barrel slice cut out



Integration in 4π Geant4 IDEA simulation (endcap)

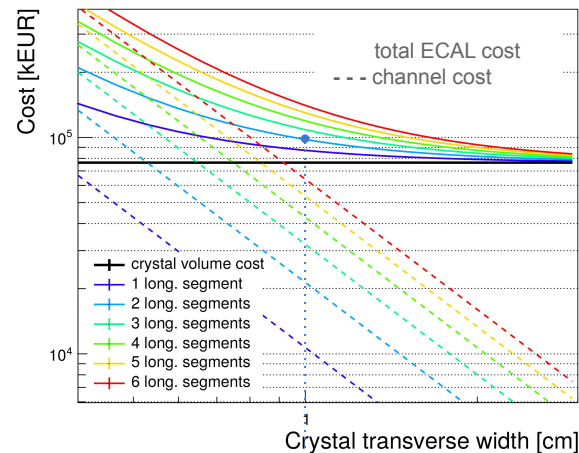
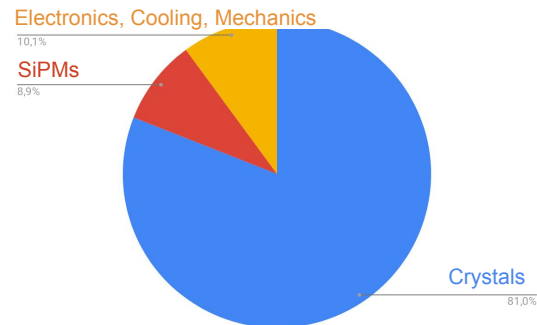
- Concentric pointing rings
- Each ring divided in replicas to yield similar crystal dimensions



More on cost/performance optimization

Cost-power drivers and optimization

- **Channel count in SCEPCal is limited to ~2.5M**
 - 625k channels/layer (2 “timing layers” + “ECAL layers”)
- Cost drivers in **ECAL** layers (tot ~95M€):
 - **~81% crystals**, 9% SiPMs, 10% (electronics+cooling+mechanics)
 - **~19% of cost scales with channel count**
- Power budget driven by electronics: ~74 kW
 - 18.5 kW/layer
- Room for fine tuning of the segmentation and of the detector performance/cost optimization (see backup)



Reference design:
1 cm², 2 segments
cost ~ 95M€

Detector **cost** drivers

- **Crystal options**

- LYSO:Ce for timing layer (optimal choice for the CMS MTD)
- PWO (very compact - CMS and PANDA ECALs preferred choice)
- Many other crystals on the market may allow further optimization

- **Crystal costs used as reference**

- Quotes from crystal vendors
 - **PWO: ~7€ /cc** (for 10 m³, cut and polished)
 - **LYSO: ~30€ /cc** (for cut, polished and wrapped elements)

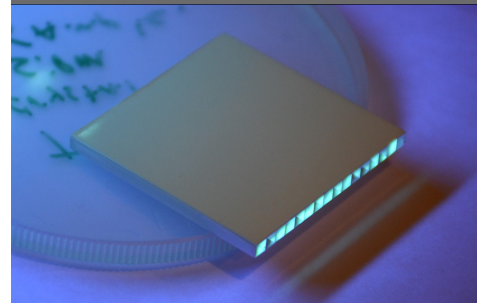
- **SiPMs**

- Recent estimates from CMS Upgrade experience:
 - **~6€/SiPM** (9x9 mm² active area)
 - can embed a LED for monitoring: additional ~1€/channel
- Cost constantly dropping and technology improving in the last decade
 - can aim at a factor ~2-4 reduction in the next decade

CMS ECAL PWO crystals



Array of LYSO crystal bars



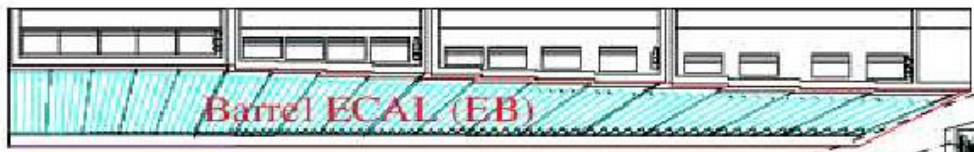
Cost and power breakdowns for SCEPCal

	T1+T2 (TIMING)	E1+E2 (ECAL)
Area barrel	53	53
Area endcap	19	19
Total area (barrel+endcaps)	72 m²	72 m²
# Channels barrel	977k	859k
# Channels endcaps	344k	374k
Total # of channels (barrel + endcaps)	1.3 M	1.2 M
Crystal cost	10 M€	78 M€
SiPM cost (+monitoring for ECAL only)	8 M€	8.5 M€
Electronics cost	5 M€	4.5 M€
Cooling+power+mechanics cost	5 M€	5 M€
Sub-total cost (barrel+endcaps)	28 M€	96 M€
Total cost (barrel+endcaps)	~124 M€	

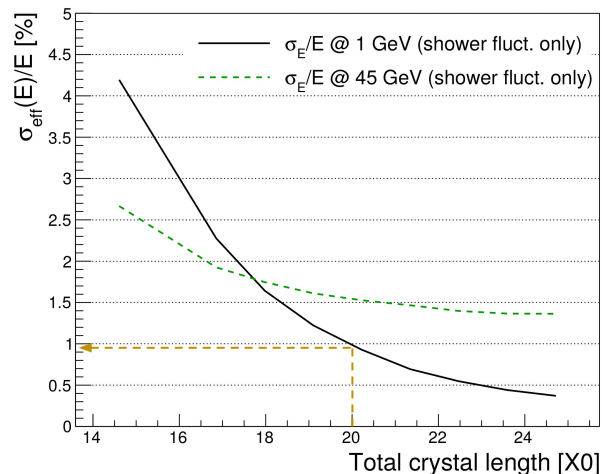
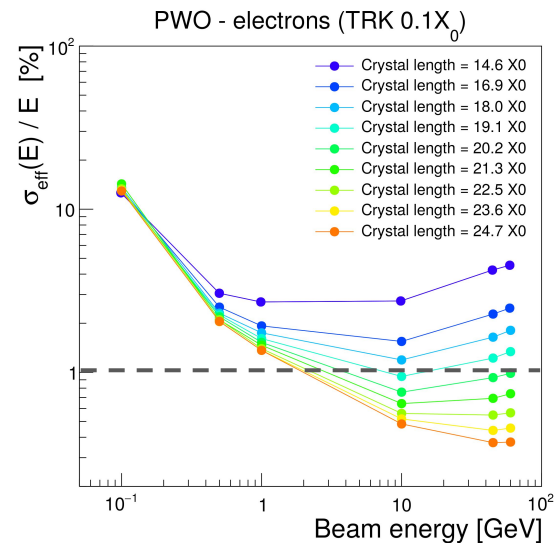
	T1+T2 (TIMING)	E1+E2 (ECAL)
# of readout channels	~1.3M	~1.2M
SiPMs (kW)	2.7	2.5
Electronics (kW)	34.3	33.5
Sub-total (kW)	38	36
Total (kW)	~74 kW	

Optimization of crystal volume

- Crystal pointing geometry
→ reduce by ~20% crystal volume and channel count

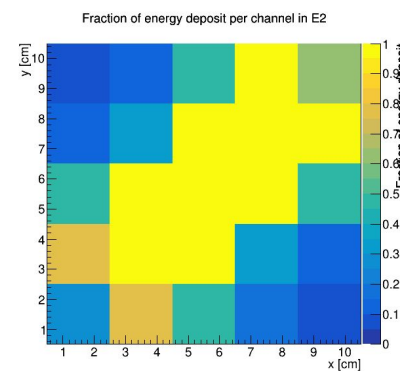
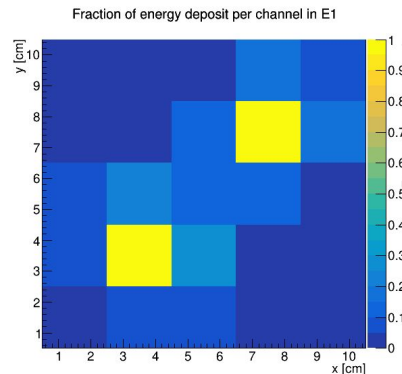


- Optimizing crystal length vs energy resolution
 - with $20 X_0$ contribution to constant term from shower leakage comparable to intercalibration precision: $O(1\%)$
 - no substantial impact on stochastic component (negligible wrt photo-statistics term of ~4-5%)

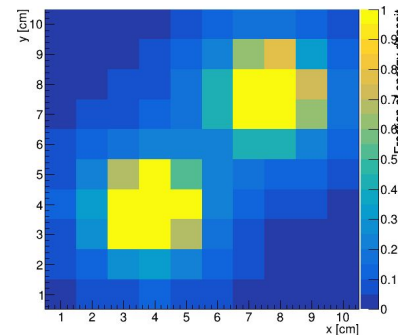
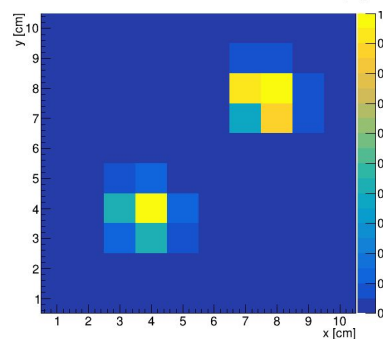


Transverse segmentation (visual impact)

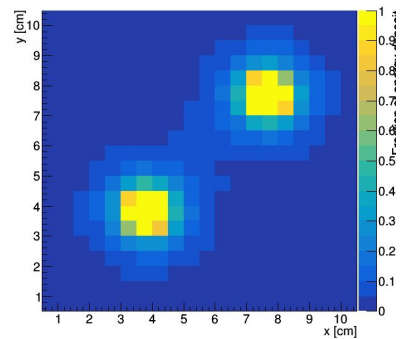
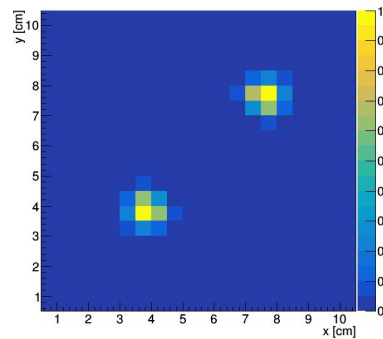
cell size: $2 \times 2 \text{ cm}^2$



cell size: $1 \times 1 \text{ cm}^2$

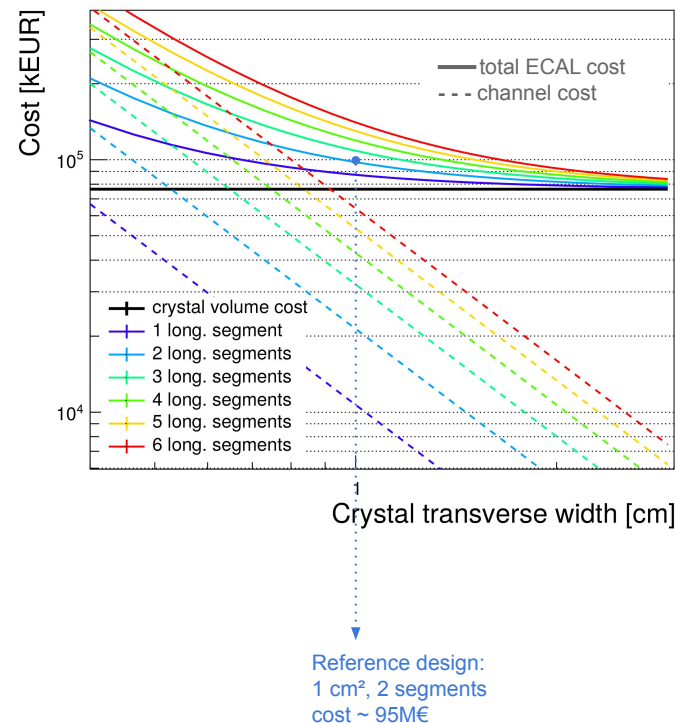


cell size: $0.5 \times 0.5 \text{ cm}^2$



Optimization of segmentation

- Segmentation optimized for performance/cost:
 - **Transverse** segmentation:
 - 1 cm $\sim R_M / 2$ (half Molière radius)
 - **Longitudinal** segmentation: 2 segments
 - particle ID with no dead material at shower max
 - simple for readout and services (front and rear)
- Impact of ch. count on overall detector cost <20% for baseline segmentation choice
- Total cost ~ 95 M€



More on dual-readout implementation

Implementing dual readout in crystals

- First test of combination of a DRO crystal ECAL with DREAM HCAL back in 2009 with BGO modules ([N.Ackurin et al., NIM A 610 \(2009\) 488-501](#))

Successful demonstration that DRO principles also apply to a hybrid calorimeter system (despite many experimental limitations!)

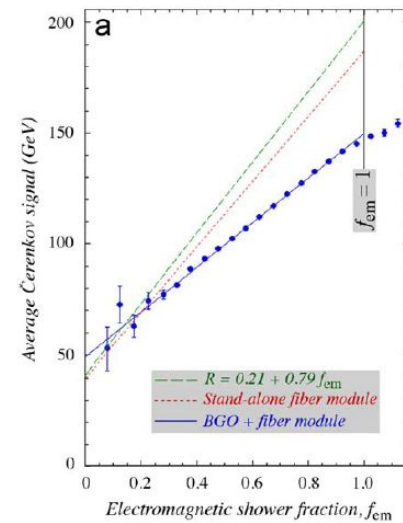
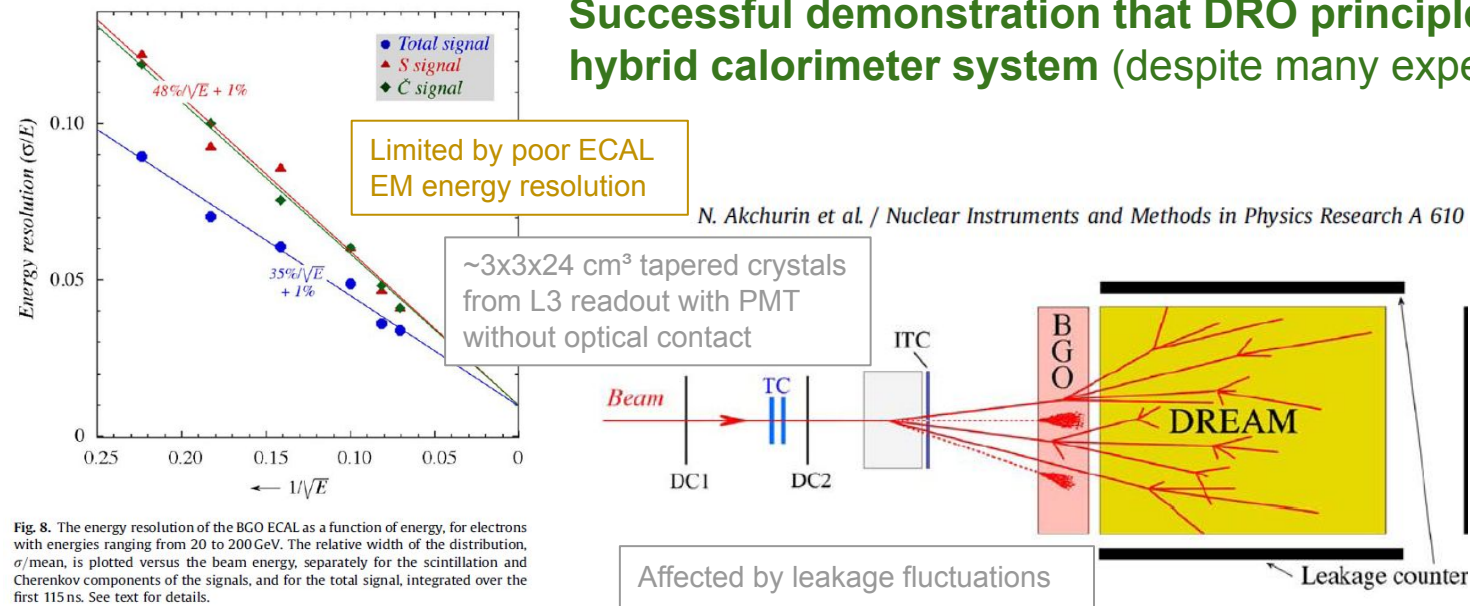


Fig. 8. The energy resolution of the BGO ECAL as a function of energy, for electrons with energies ranging from 20 to 200 GeV. The relative width of the distribution, σ/mean , is plotted versus the beam energy, separately for the scintillation and Cherenkov components of the signals, and for the total signal, integrated over the first 115 ns. See text for details.

DRO in the rear SCEPCal segment **only**

- Majority of the energy deposit from hadron is in the rear ECAL section
- Dual readout can be implemented in the rear section only**
 - No degradation in performance wrt a full (front+rear) DRO ECAL
 - +50% in channel count wrt to non-DRO ECAL can be mitigated by decreasing granularity in the rear compartment where shower radius is larger

doubling SiPMs for DRO
only in the rear section

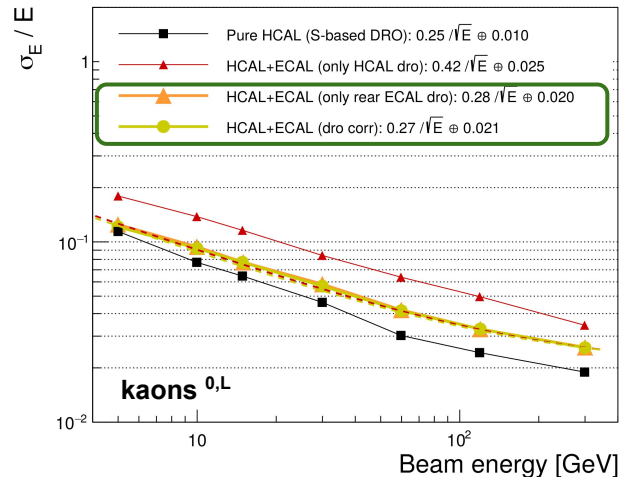
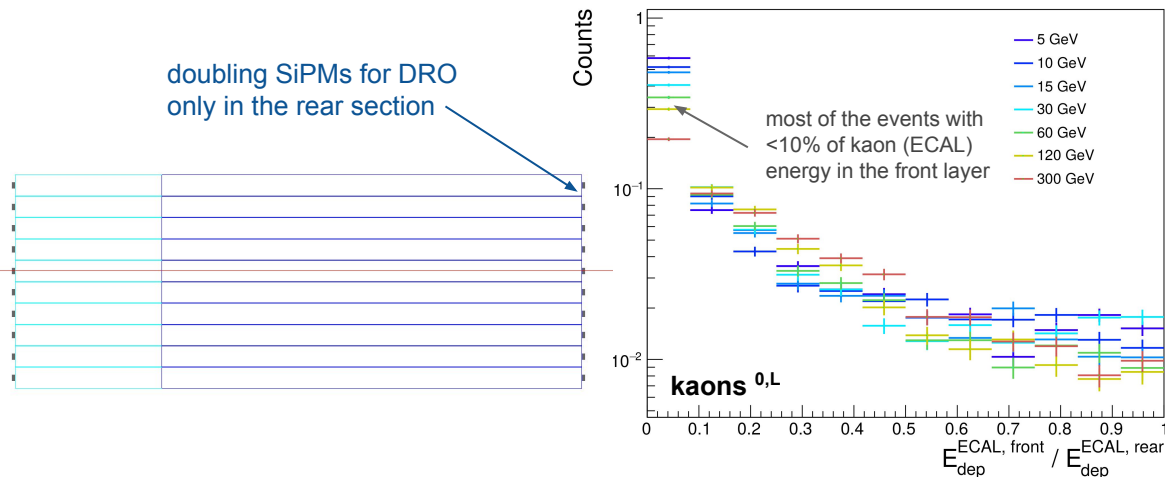
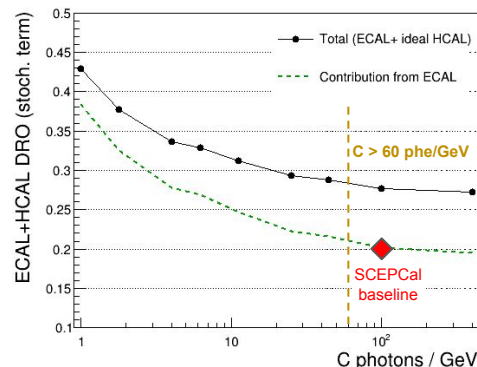
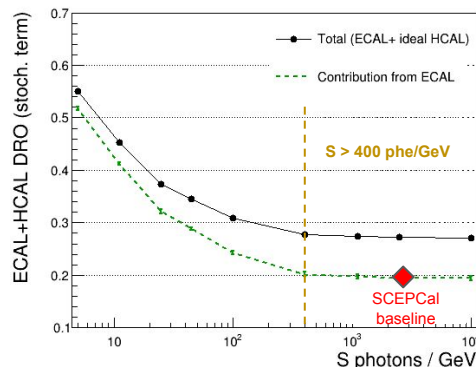
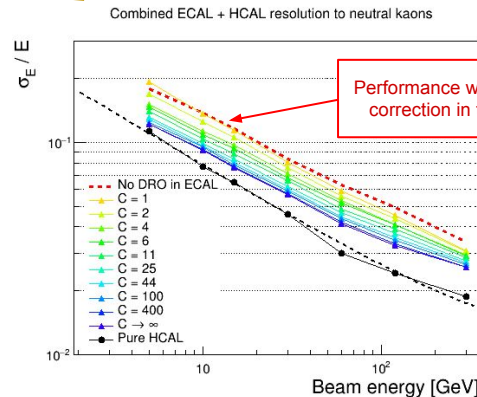
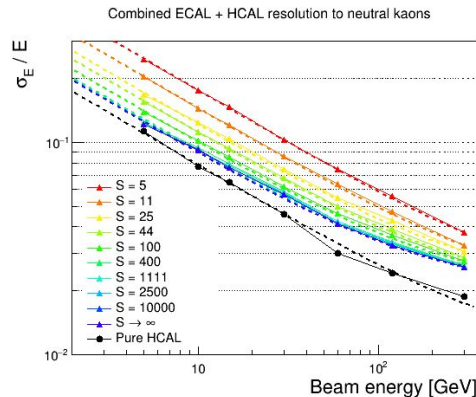


Photo-statistic requirements for S and C

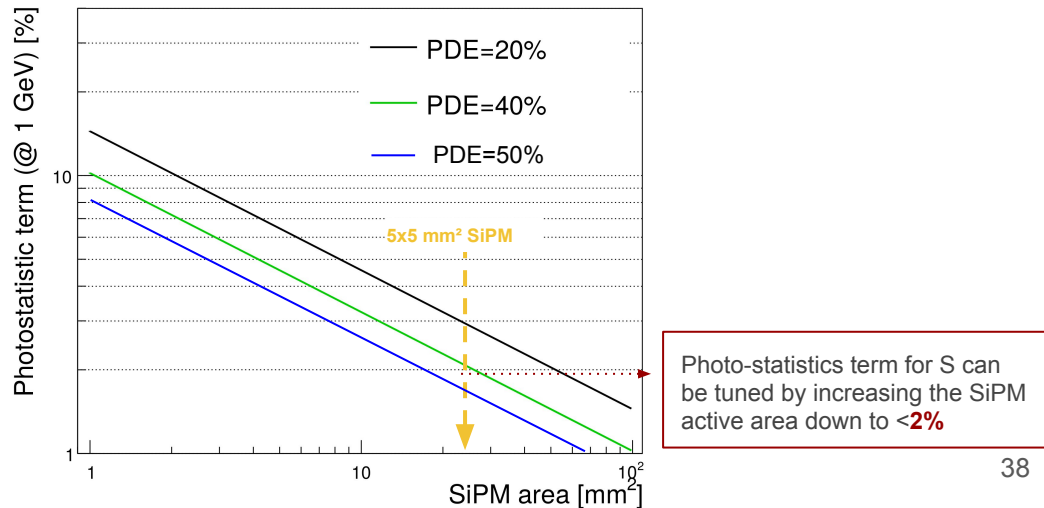
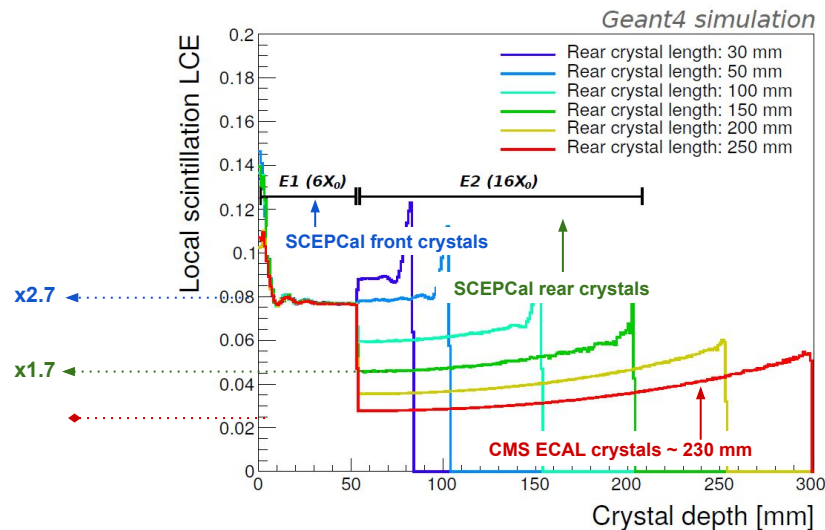
Smearing according to Poisson statistics

- Poor S directly impact the ECAL resolution stochastic term (even without DRO):
 - $S > 400$ phe/GeV to limit the contribution to HCAL stoch. term below 20%
- A limited resolution to C (photostatistics) impacts the C/S and thus the precision of the event-by-event DRO correction
 - $C > 60$ phe/GeV to limit the contribution to HCAL stoch. term below 20%



SCEPCal key features for DRO optimization

- **High granularity increases light collection efficiency** (both C and S)
 - 1 cm² cross section compared to ~ 3 cm² in L3/CMS and crystal length reduced by ~2x
- **SiPM active area can be tuned** to achieve target resolution (stoch. term)
 - Light collection efficiency increasing linearly with SiPM area
- SiPM with smaller dynamic range but high PDE can be selected for C-detection



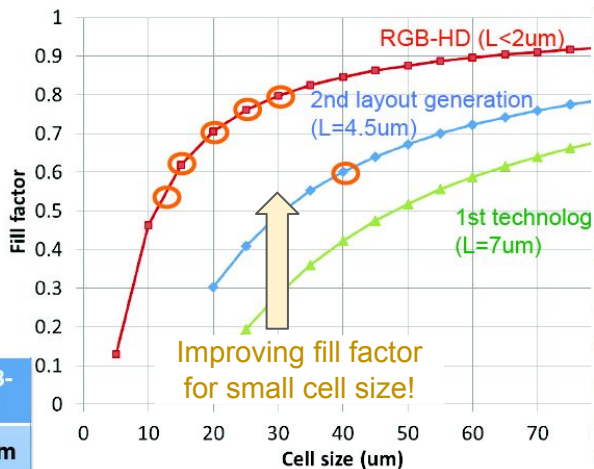
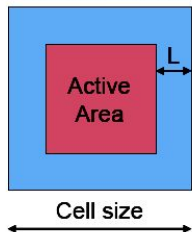
Technological advancements (SiPMs)

- Many technological advancements in the field of photodetectors
- Compact and robust SiPMs with **small cell size and fast recharge time** (~ 4 ns) **extending the dynamic range and enhancing sensitivity** in a wide range of wavelengths

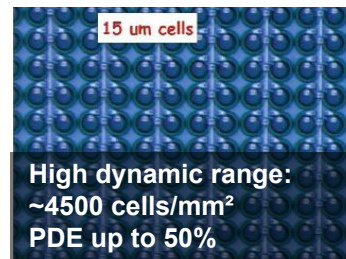
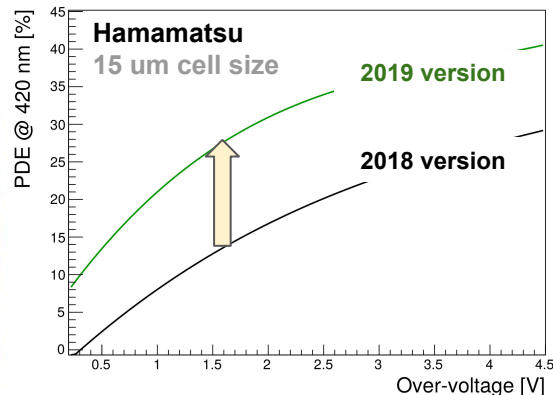
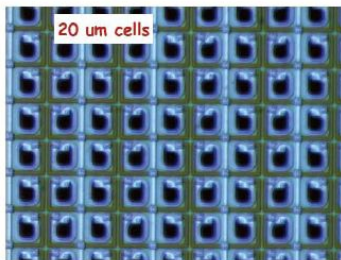
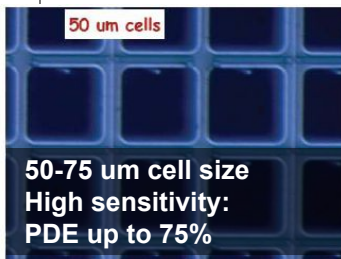


RGB-HD SiPM technology

SiPM Cell, top view



	Std. SiPM RBG	RGB- HD
CS	40 μm	15 μm
FF	60 %	62 %



Validation of Geant4 ray-tracing simulation

- Geant4 simulation for ray-tracing of Cherenkov photons validated
- **Reproducing experimental results from test beam**

(thanks to G.Gaudio for help in retrieving details of the setup!)

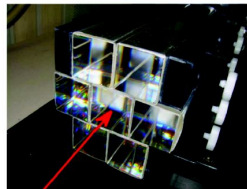


Fig. 2. The PWO matrix consisted of seven crystals with dimensions of $3 \times 3 \times 20 \text{ cm}^3$. These were arranged as shown in the figure and the beam entered the matrix in the central crystal. All crystals were individually wrapped in aluminized mylar. Both the upstream and downstream end faces were covered with filters. See text for details.

F. Bedeschi, G. Gaudio, et al. <https://www.sciencedirect.com/science/article/pii/S0168900212014520>

Geometry and material description in the paper

- 7 crystals with dimensions of $30 \times 30 \times 200 \text{ mm}^3$
- All crystals were individually wrapped in aluminized mylar.
- Hamamatsu R8900-100 tubes
- Both the upstream and downstream end faces of the matrix were covered with a large optical transmission filter (U330 or UG5)
- Silicone cookies were used to reduce the light trapping effect

PMT1

PMT2

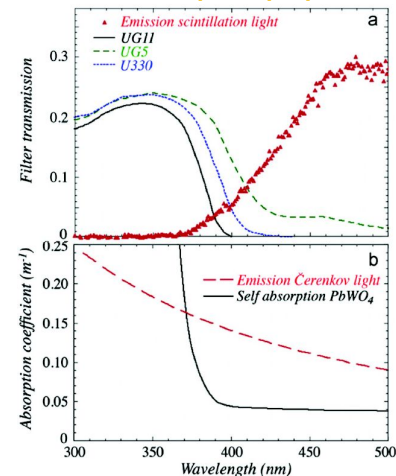
PMT
 $25 \times 25 \times 5 \text{ mm}^3$

Silicone gap
refrac_idx 1.403
 $25 \times 25 \times 0.1 \text{ mm}^3$

PMT window
refrac_idx 1.525
 $25 \times 25 \times 0.8 \text{ mm}^3$

- Crystal wrapped with aluminum sheet of 0.985 reflectivity
- 0.1 mm silicone gap between crystal and PMT Borosilicate glass window
- Interface between gap and PMT window is set as the filter
- PMT surface is set as sensitive

Simulation of optical filters and PWO optical properties

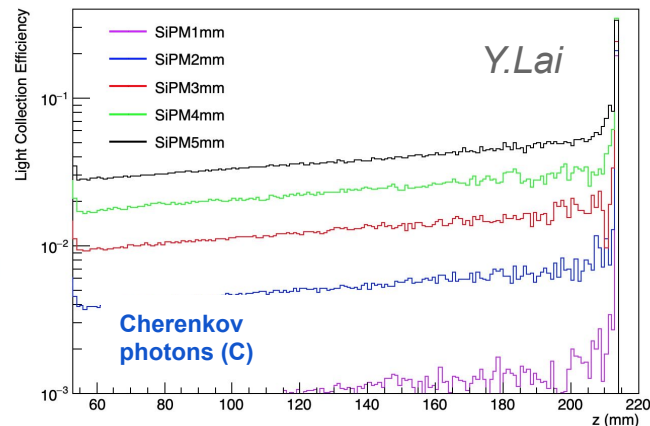
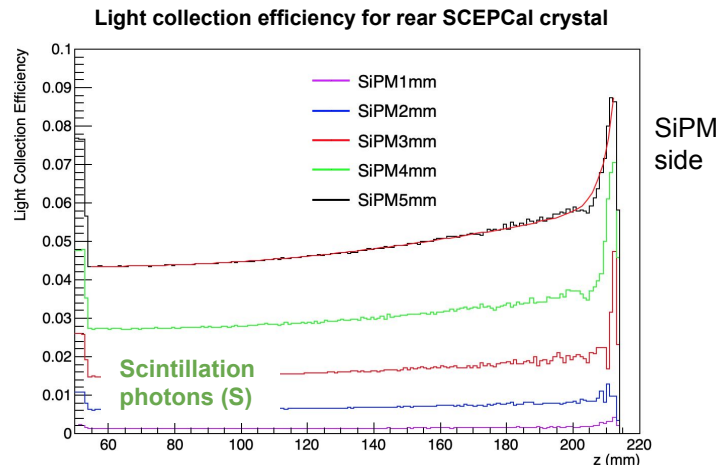
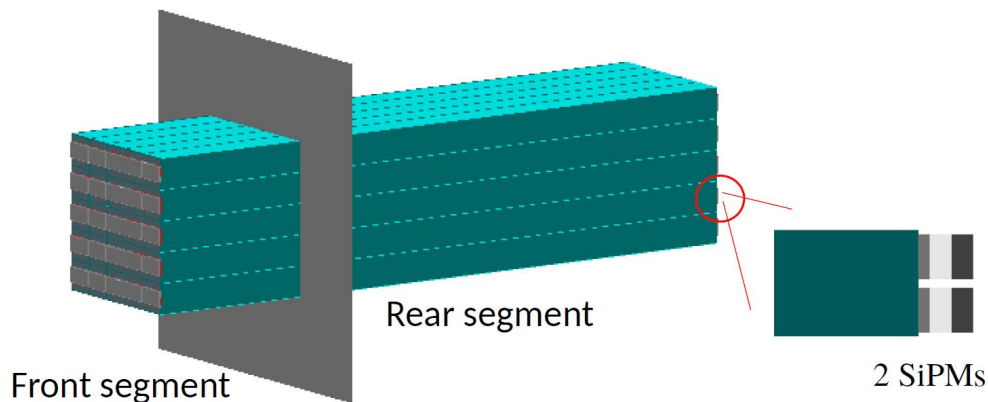


MC to data comparison: simulation predicting ~40% more Cherenkov photons (fine tuning ongoing)

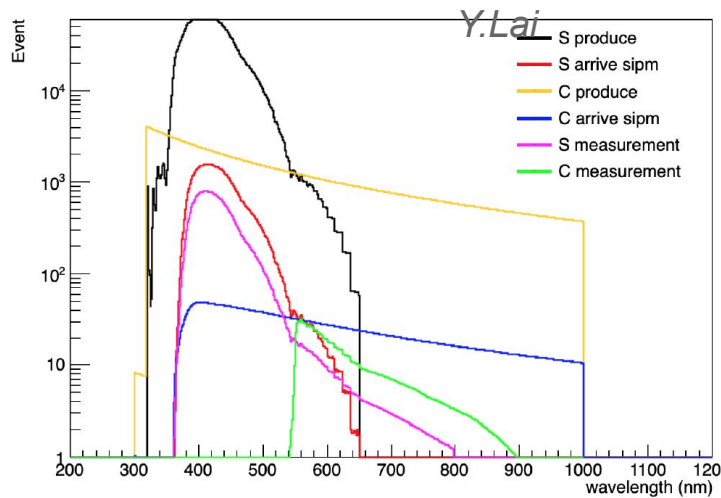
Filters	Detected photons (50 GeV e ⁻)		Number in paper (50 GeV e ⁻)
	Upstream	downstream	
No filter /No filter	9950	14860	
No filter/U330	9146	781	
No filter/UG5	9199	1278	
U330/U330	517	774	650
U330/UG5	513	1246	1250

Ray-tracing in the SCEPCal

- Study impact of various parameters on light collection efficiency for both S and C:
 - LCE grows linearly with SiPM active area
 - LCE grows with shorter crystals



Fraction of S and C photons detected with dual SiPM



- RGB and UV SiPM are used to detect Cherenkov and scintillation photons
- All the photons detected by UV SiPM are considered as S
- The 550nm filter is added to RGB SiPM, so only photons with wavelength $> 550\text{nm}$ could be detected. In this region, C is dominant
- The left plot shows spectrum of S and C when they are produced, arrived at the end and collected by SiPM
- The number of photons at different stages are shown in the table below, but it is a rough estimate, as the scintillation spectrum we are using is clearly rough up when wavelengths $> 550\text{nm}$.

Table 2. Photon yield for both Cherenkov and scintillation light in response to a 45 GeV electron shower in the rear SCEPCal segment assuming a PbWO_4 crystal and the SiPM spectral sensitivity shown in Figure 24 (left).

	Scintillation [photons/GeV]	f_S [%]	Cherenkov [photons/GeV]	f_C [%]
Generated	200000	100	56000	100
Collected	10000	5.0	2130	3.8
Detected by NUV SiPM #1 ($\lambda < 550\text{ nm}$)	2000	1.0	140	0.25
Detected by RGB SiPM #2 ($\lambda > 550\text{ nm}$)	< 20	< 0.01	160	0.3

Increase of C/S ratio in irradiated PWO crystals

- **An example of high wavelength Cherenkov detection**

- Radiation damage in PWO crystals filtering out the scintillation and enhancing the relative contribution of C photon (with $\lambda > 500$ nm) to the signal
- Pulse shapes also get faster

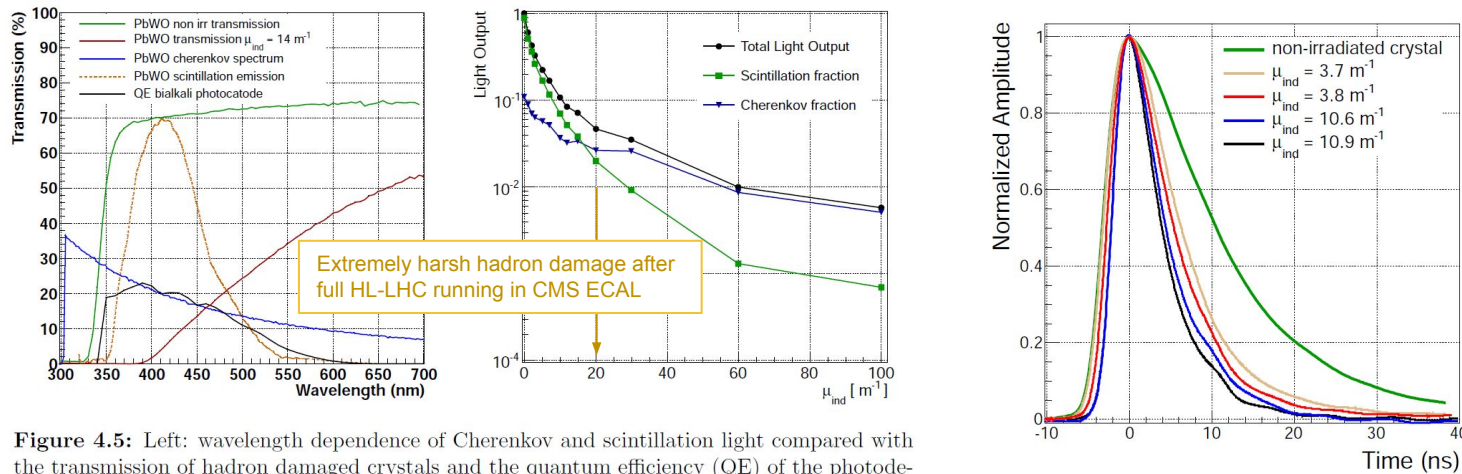
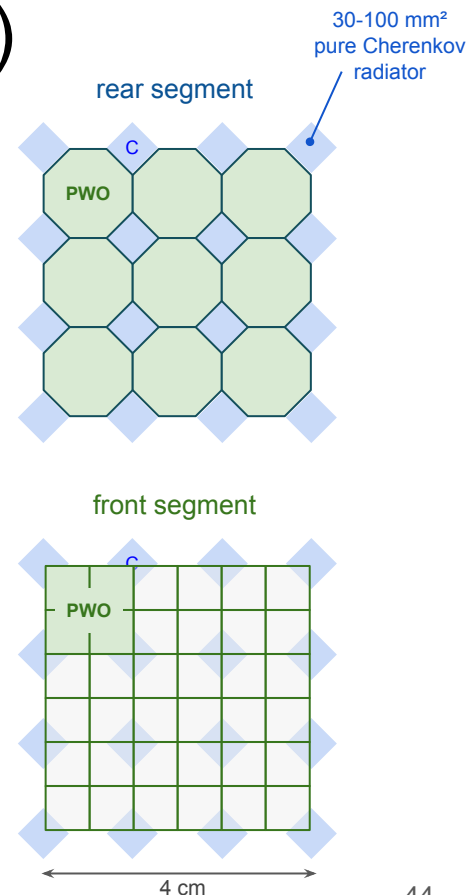


Figure 4.5: Left: wavelength dependence of Cherenkov and scintillation light compared with the transmission of hadron damaged crystals and the quantum efficiency (QE) of the photodetector. Right: contribution of scintillation and Cherenkov signal to the total light output at different μ_{ind} .

Dedicated **C-sensitive** elements (option)

- A ‘honeycomb’ structure for the rear crystal section
 - Pure Cherenkov radiators nested with scintillating crystals
 - C and S elements individually readout with SiPMs
 - Size of C-element can be optimized to achieve good C “sampling”
- Front SCEPCal segment unchanged:
 - Pure S-crystal with 1 cm² → no projective cracks
- Reduce transverse segmentation in the rear segment by using octagonal (~1 cm side) crystals
 - Shower radius is larger in the rear section (less segmentation needed)
 - Total SCEPCal channel count reduced by ~25%

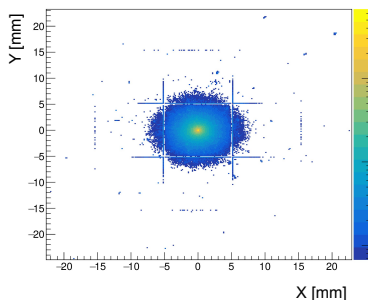


C-only DRO optimization (work in progress)

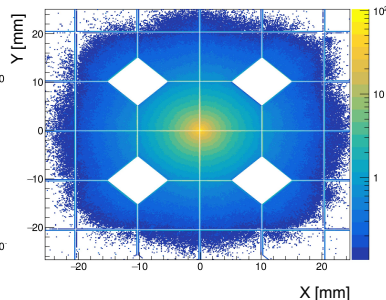
- Design under optimization
 - Tuning granularity and dimensions of C sensitive material
 - Choice of C-radiator (e.g. quartz vs undoped crystal)
- Optimize C-sampling fraction vs resolution to EM particles

Energy deposits in active elements (except ECAL C-radiator)

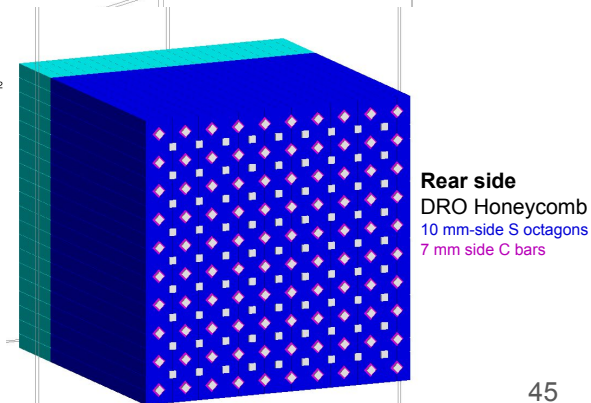
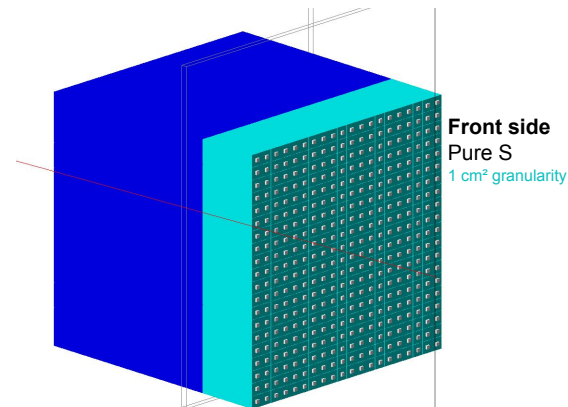
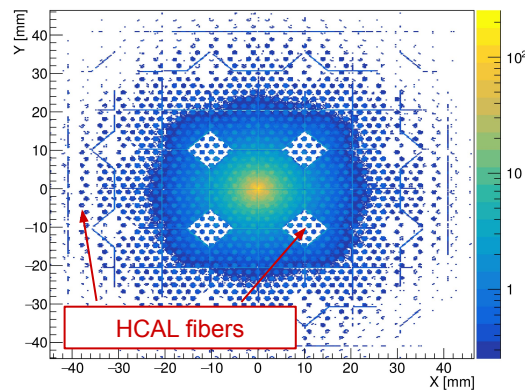
front ECAL layer



rear ECAL layer



ECAL+ HCAL



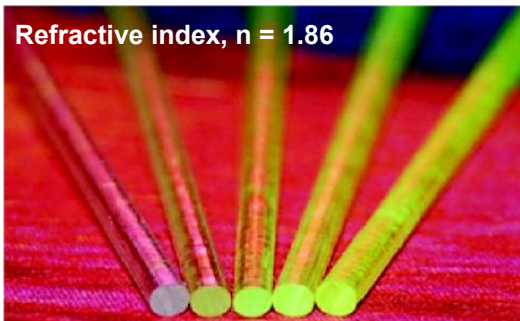
Crystal based Spaghetti Calorimeters

- Technology wise, a lot of progress in high granularity crystal calorimeters
 - New materials and new production processes
 - **Undoped LuAG crystals as excellent cherenkov radiators**
 - Crystal based SPACAL being studied for LHCb HL-LHC upgrade

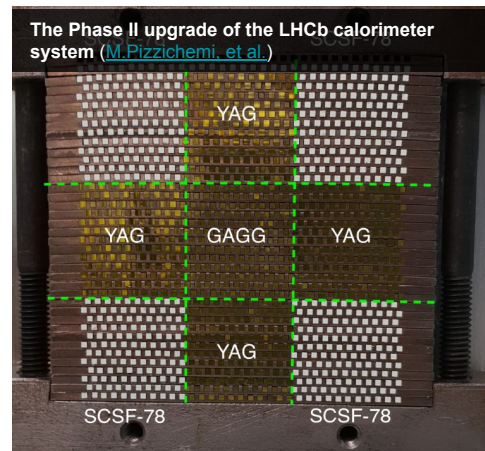
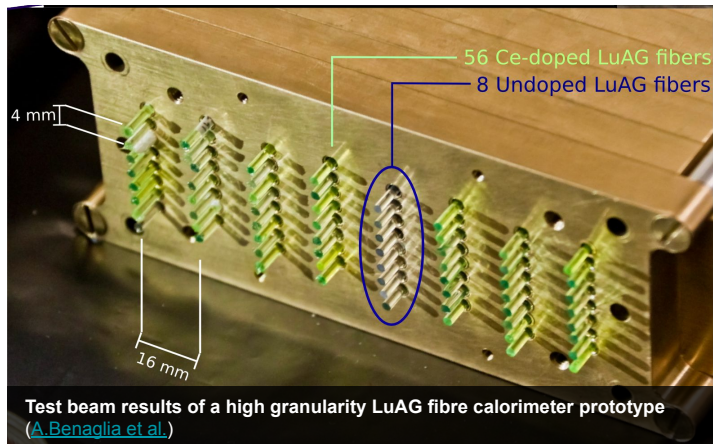
$\text{Lu}_3\text{Al}_5\text{O}_{12}$
 $\rho = 6.73 \text{ g/cm}^3$
 $X_0 = 1.41 \text{ cm}$
 $\lambda_1 = 23.3 \text{ cm}$

Undoped:
Cherenkov radiator
Cerium-doped:
Good scintillator

Refractive index, $n = 1.86$

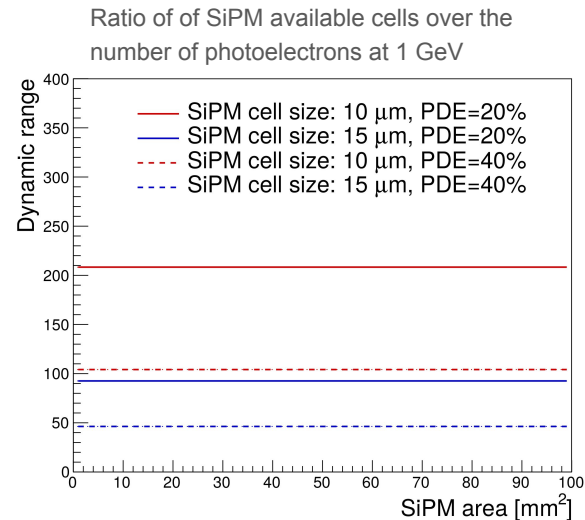
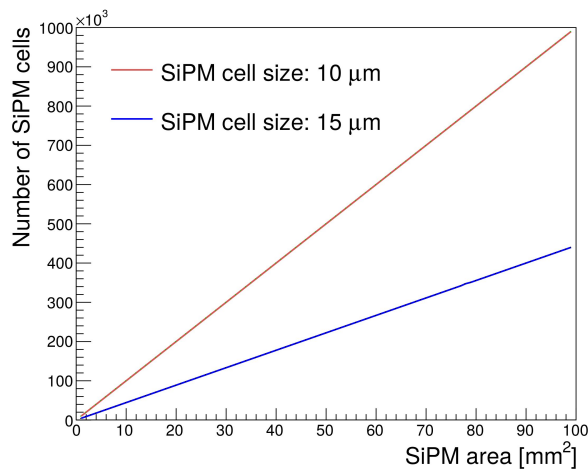
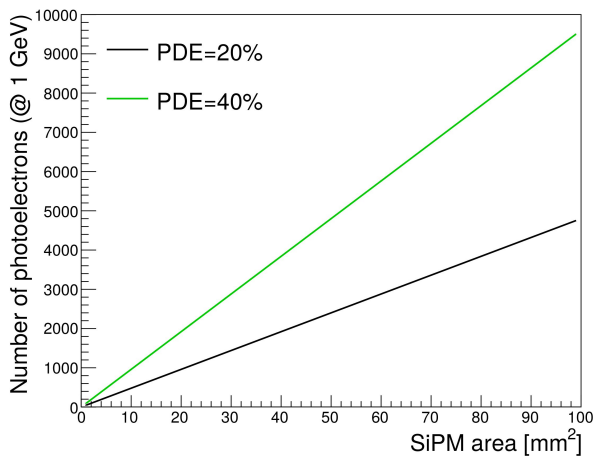


Formerly [proposed](#) for “Studies on sampling and homogeneous dual readout calorimetry with meta-crystals”



Dynamic range with SiPMs

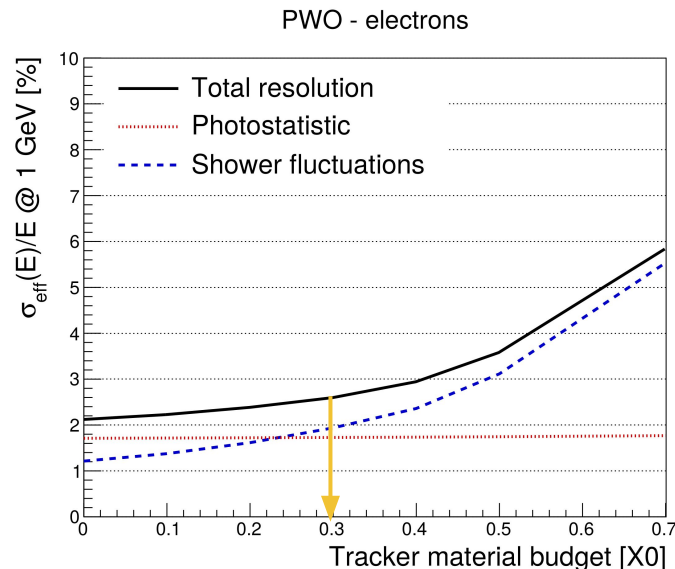
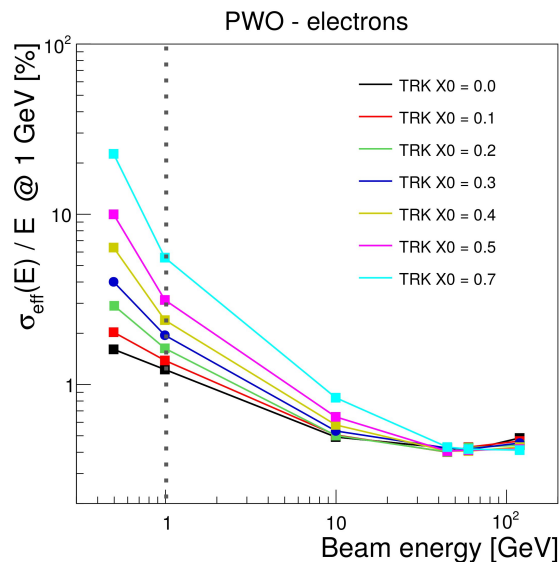
- 15 μm cell pitch has high PDE (up to 50%) \rightarrow optimal for T1 and T2 (timing)
- 10 μm cell pitch has larger dynamic range \rightarrow possibly better for E1, E2 (ECAL)



More on ECAL and HCAL performance simulation

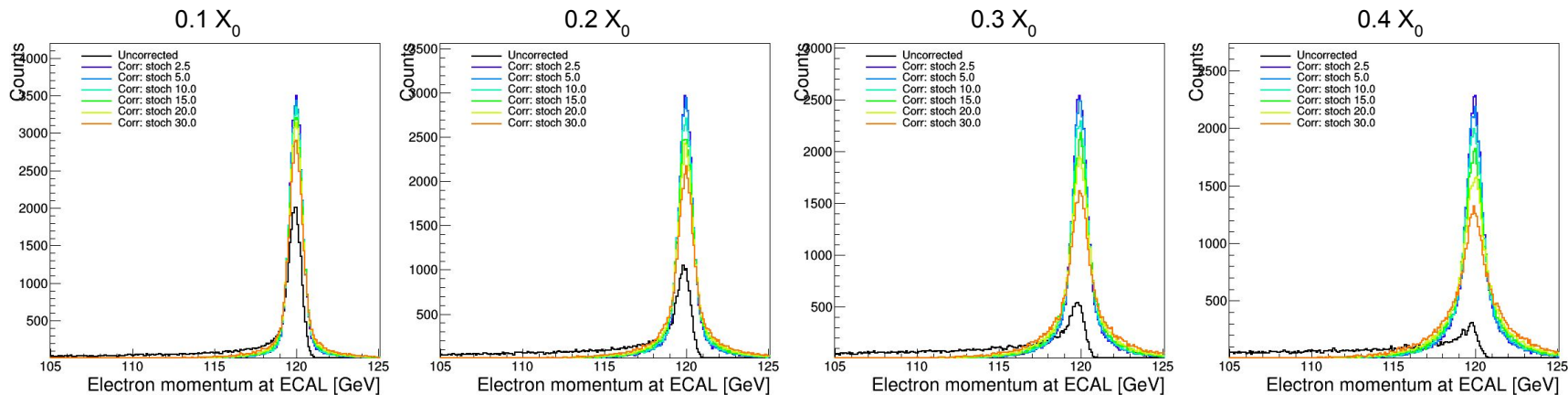
Impact of tracker and dead material budget

- Tracker material budget $< 0.3X_0$ for $< 2\%$ impact on stoch. term
 - Well within the target of the CEPC and IDEA reference tracker designs
- Dead material for services $< 0.3X_0$ for impact on stoch. term $< 2\%$
 - Compatible with estimated material budget from cooling (5 mm Al plate) and readout electronics



Recovery of Bremsstrahlung photons (1)

- Electron momentum at the entrance of ECAL smeared by 0.3 %
- 120 GeV electrons
- Adding back brem photons with ECAL resolution



Recovery of Bremsstrahlung photons (2)

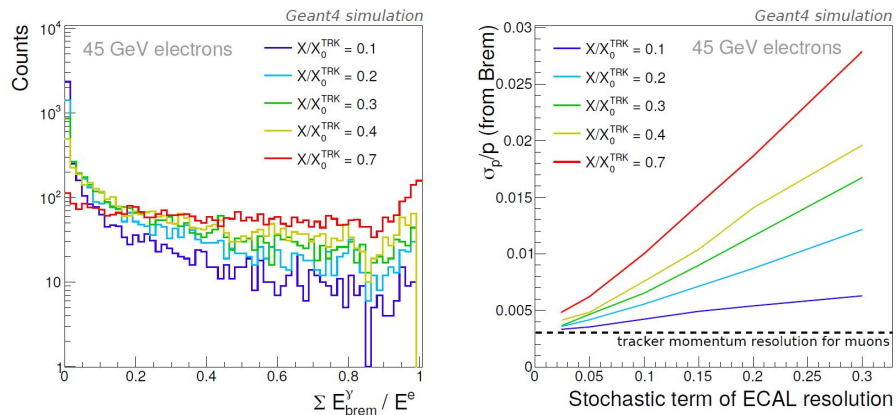


Figure 3. Left: fraction of the total energy lost by 45 GeV electrons through bremsstrahlung radiation within the tracker volume (before reaching the calorimeter) for different scenarios of tracker material budget. Right: contribution to the resolution of the electron momentum at vertex due to bremsstrahlung assuming the energy of photons emitted within the tracker volume are measured by calorimeter with a certain stochastic term of energy resolution.

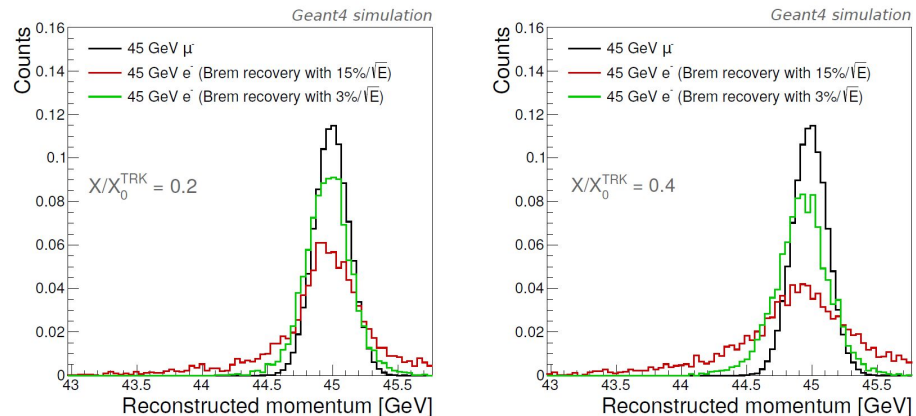
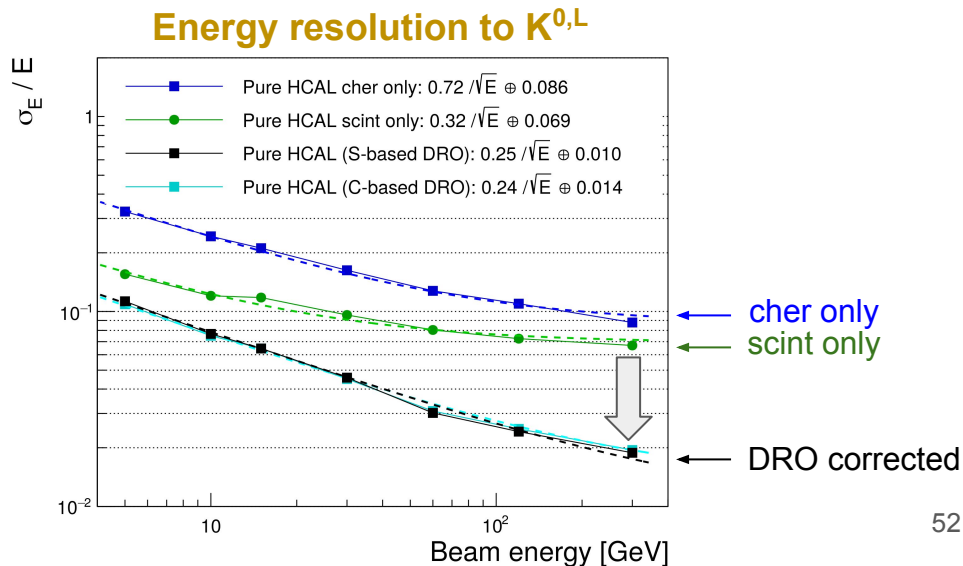
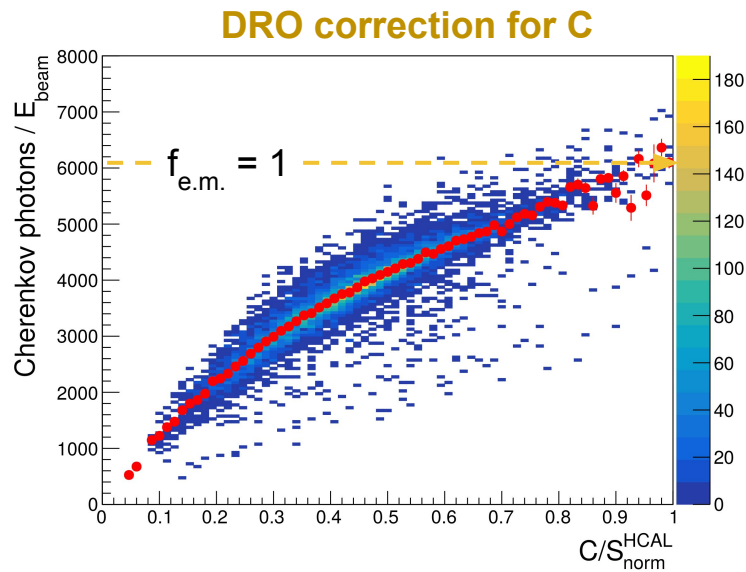


Figure 4. Distributions of the reconstructed momentum for muons (assuming a tracker momentum resolution of 0.3%) and for electrons assuming recovery of bremsstrahlung photons with an energy resolution of $15\%/\sqrt{E}$ and $3\%/\sqrt{E}$. Two scenarios are shown: assuming a tracker material budget equivalent to 0.2 X_0 (left) and 0.4 X_0 (right).

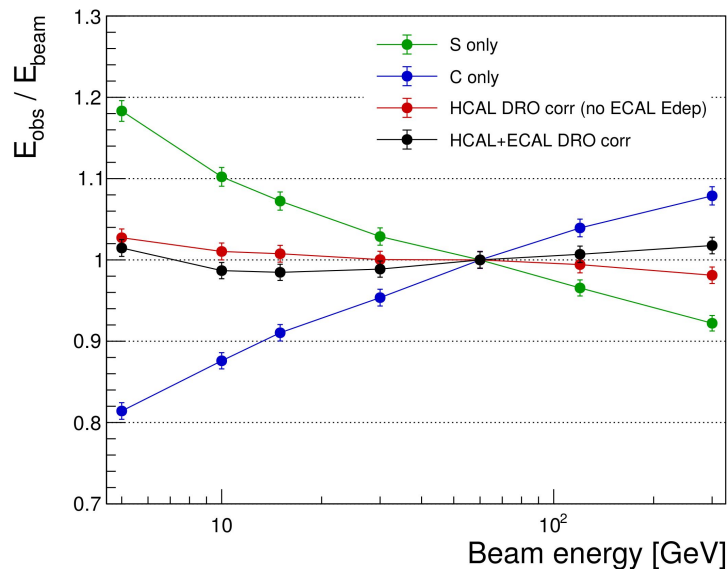
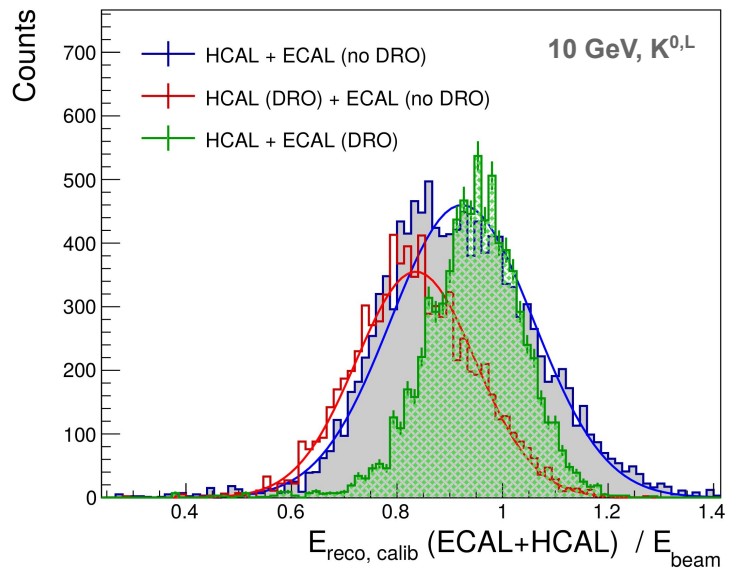
Performance of the dual readout HCAL only

- Performance studied by selecting events with hadrons that do not interact in the crystal
- **Dual readout correction works as expected**
 - Energy resolution of $\sim 25\%/\sqrt{E} \oplus 1\%$ to hadrons
 - Linearity and gaussian distributions restored

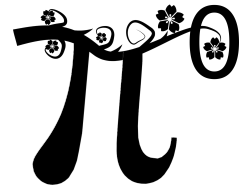


Linearity (SCEPCal + DRO HCAL)

- Gaussian distributions and response linearity restored



Maximum weight matching via Blossom V algorithm
for π^0 reconstruction in multi-jet events



Algorithm

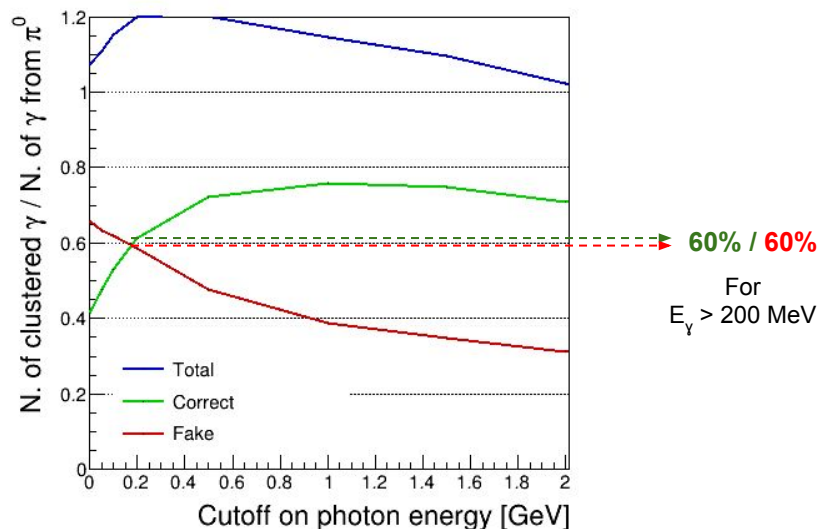
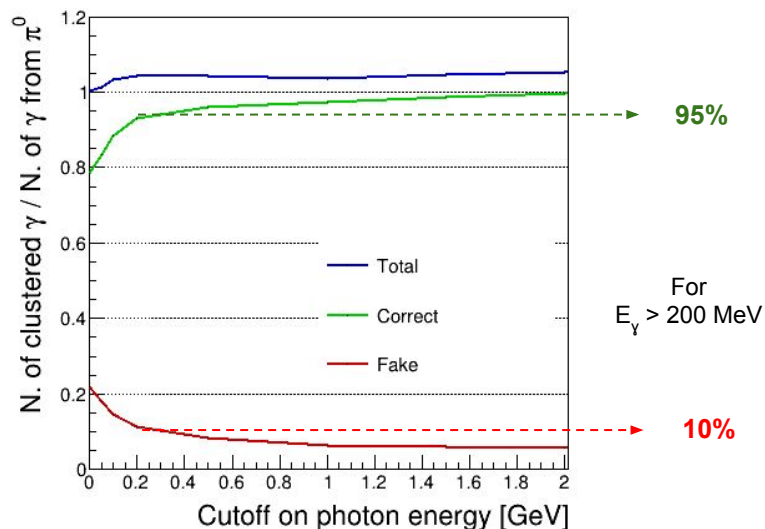


NetworkX
Network Analysis in Python

- [max_weight_matching](#) (*G*, *maxcardinality=False*, *weight='weight'*)
- Compute a maximum-weighted matching of *G*.
 - A matching is a subset of edges in which no node occurs more than once.
 - The weight of a matching is the sum of the weights of its edges.
 - A maximal matching cannot add more edges and still be a matching.
 - The cardinality of a matching is the number of matched edges.
- If *G* has edges with weight attributes the edge data are used as weight values else the weights are assumed to be 1.
- This function takes time $O(\text{number_of_nodes} ** 3)$.
- This method is based on the “blossom” method for finding augmenting paths and the “primal-dual” method for finding a matching of maximum weight, both methods invented by Jack Edmonds [1].

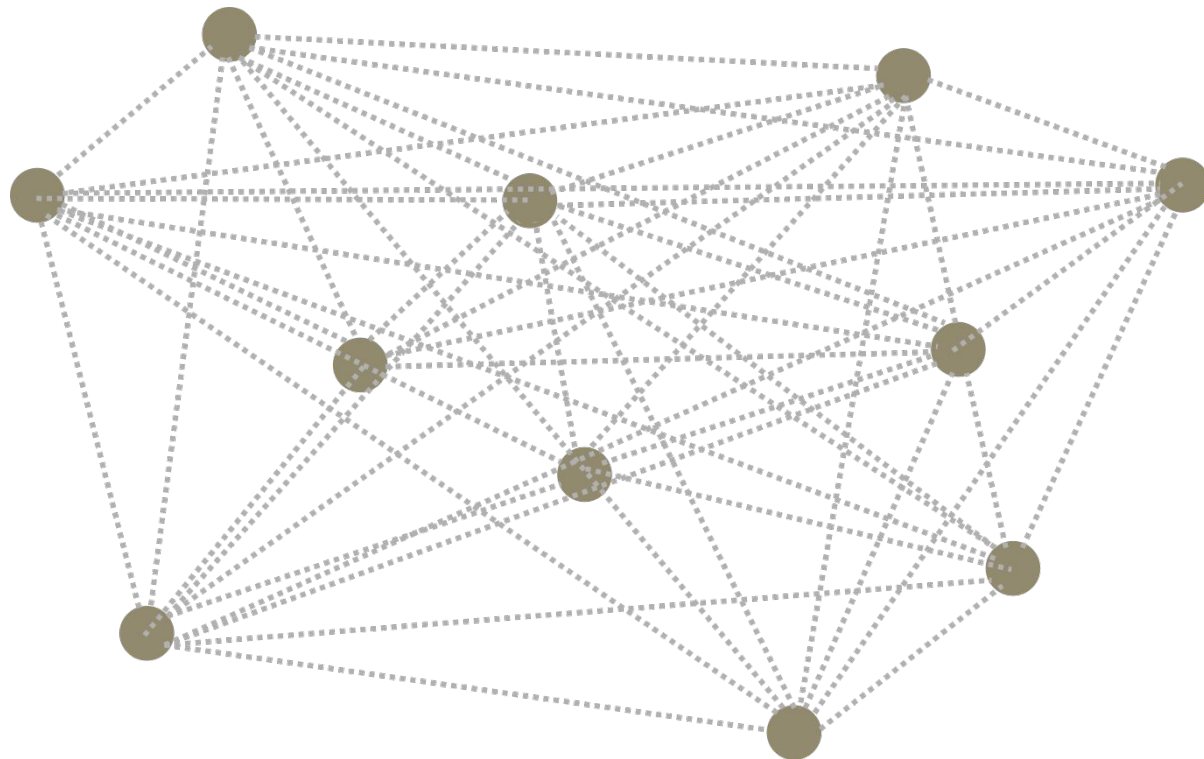
Algo performance vs photon energy cut (results)

- Close to 100% of π^0 's with both photons with energy >200 MeV correctly reconstructed with $3\%/\sqrt{(E)}$ resolution



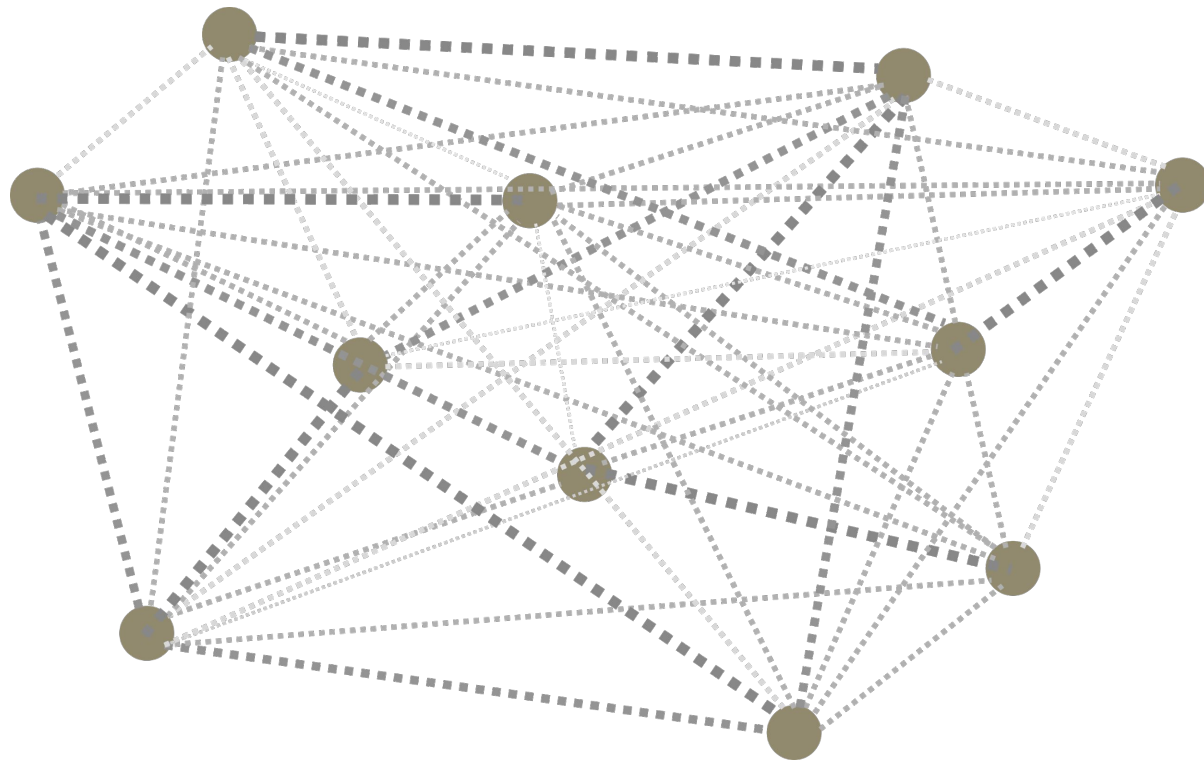
Building graph

- **node** = photon
 - **edge** = pair of photons
-
- node properties
 - p_x, p_y, p_z, E
 - edge properties
 - invariant mass
 - boost
 - angle



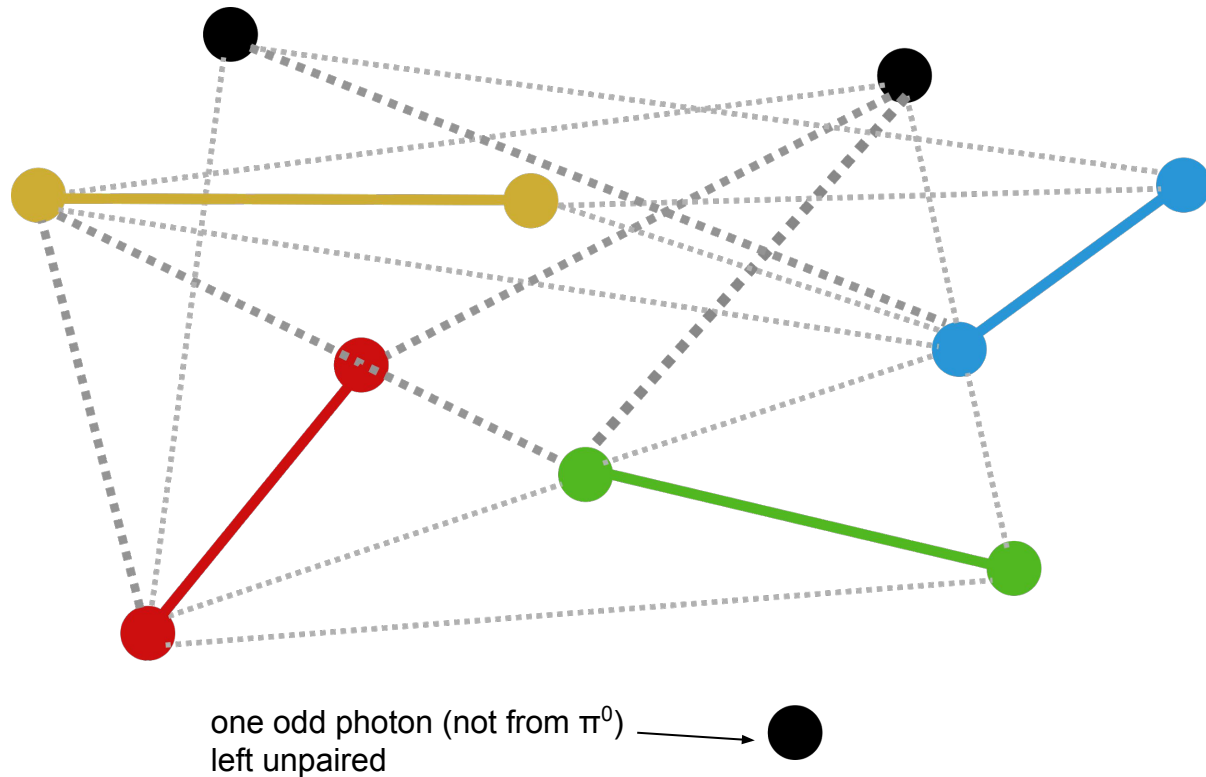
Assigning weights

- Assign a **weight**, w_{ij} , to each edge
- $\chi^2_{ij} = (M_{y,i y,j} - M_{\pi})^2 / M_{\pi}$
- $w_{ij} = 1 - \chi^2_{ij} / \chi^2_{\max}$
- $\chi^2_{\max} = \max(\chi^2_{ij})$
- $w_{ij} \in [0,1]$



Comments on solution

- black dots = photons that do not originate from a π^0 decay
- Hard cut on ‘structure’ may reduce to substantially the fraction of wrong photon pairing from photons not from π^0 decays (“spare photons”)



Example of CNN structure with 3 longitudinal layers

